FEASIBILITY OF DETECTING SANDSTONE LENSES IN THE DAKOTA FORMATION BY SEISMIC REFLECTION, RUSSELL AND ELLIS COUNTIES, KANSAS

by

William George Coyle III
B.S. , University of New Orleans, 1986

Submitted to the Department of
Geology and the Faculty of the
Graduate School of the University
of Kansas in partial fulfillment
of the requirements for the degree
of Master of Science.

Chairman

Committee Members

For the Department

Date thesis accepted

Kansas Geological Survey
Open-file Report

Disclaimer

The Kansas Geological Survey does not guarantee this document to be free from errors or inaccuracies and disclaims any responsibility or liability for interpretations based on data used in the production of this document or decisions based thereon. This report is intended to make results of research available at the earliest possible date, but is not intended to constitute final or formal publication.

Abstract

I determined that shallow reflection seismology can be used to locate shallow sandstone lenses in the Dakota Formation. I used walkaway noise tests to select acquisition parameters for four CDP seismic lines. The lines where shot in a variety of near-surface conditions and at different stratigraphic levels above the Dakota Formation. Resolution and data quality were site dependent. Where Graneros Shale was at the surface, the resolution allowed easy recognition of the top and bottom of the channel and beds within the Kiowa Shale. Sites with dry alluvium at the surface resulted in lower recorded frequencies and lower data quality. The channel sand was still recognizable at these sites, but the reflection from the base of the channel sand was part of a composite reflection representing acoustic impedance contrasts within the Kiowa Shale. Where the Greenhorn Limestone was at the surface, high-amplitude linear coherent noise ("ringing refractions") saturated the system and prevented the recording of reflection information. At the site located on the Carlile Shale above the Greenhorn Limestone, the channel sand could have been resolved if it had been present. At each of the sites, higher frequencies were recorded and data quality was higher when the source and receivers were located in the road ditch rather than on the road. F-k filtering can be used to remove coherent linear noise associated with shallow reflection data without creating artificial coherency. Linear moveout at the velocity to be filtered before two-dimensional Fourier transformation and smooth tapering of the fan cut filter centered on the 0 wavenumber axis were critical factors in not creating artificial coherency.

Dedication

This thesis is dedicated to my family.

Acknowledgements

I'd like to thank my advisor, Don Steeples, for giving me the opportunity to work on this project. I also thank my other committee members, Don Sprowl and Doug Walker, for their timely review of the text. Rick Miller taught me the importance of good acquisition techniques while helping guide me through the collection of the seismic data. I thank Randie Grantham, Dean Keiswetter, Paul Myers, and Alan Wade for helping me collect the seismic lines. Ross Black and Choon Park programmed the f-k filters. John Doveton helped me with the synthetic seismograms. I would like to thank Vince Hamilton and Al Macfarlane for their discussions on the stratigraphy in the study area. Loren Babcock and Mimi Braverman read the manuscript. Mark Schoneweis helped with the preparation of figures. Most of all, I want thank my wife, Darcie, for coming to Kansas with me and for her endless support through this entire adventure.

TABLE OF CONTENTS

INTRODUCTION

The purpose of this study is to determine the feasibility of using high-resolution shallow reflection seismology to determine the location of sandstone lenses in the Dakota Formation of central Kansas. Concern over future demands for fresh water in central and western Kansas has pushed the state legislature to fund research aimed at finding alternative sources of water to the Ogallala aquifer. The Kansas Geological Survey (KGS) is one of the leading state agencies in that research. The shallow Ogallala aquifer, which has historically been the main source of water in western Kansas, is being depleted by overdevelopment. The Dakota aquifer will be the next available source of water for this region (KGS, 1987). Sandstone lenses within the Terra Cotta Clay Member of the Dakota Formation are alternative sources of freshwater at some localities (Bayne et al., 1971).

Sandstones within the Dakota Formation occur as sparse lenses of variable size, making it difficult to predict their distribution (Franks, 1975; Bayne et al., 1971). Studies using well log information and cores to establish a subsurface stratigraphic framework of Lower Cretaceous formations are currently being done at the KGS. This approach is limited by the spacing of existing wells and the expense of drilling new test wells.

One channel sandstone has already been mapped using available well logs and one new test well. Two new wells, drilled by the KGS, will serve as control points to test the accuracy of the seismic methods used in this study. Synthetic seismograms are used to tie the well log information to the seismic sections and to aid in the interpretation of the reflecting events.

Four lines were shot at locations that had different near-surface conditions and were at different levels within the stratigraphic column. This should enable future researchers to predict the chances of obtaining useful

reflection information at various localities within the study area. Interpretation of each of the lines and evaluation of data quality was used to determine that detecting shallow sandstone lenses by seismic reflection is feasible and that the degree of success is site dependent.

STUDY AREA

I chose the study area because it is located close to two test wells drilled by the KGS. This provided a good comparison between the rocks and their seismic signatures. The Haberer well is located in NE sec. 14, T. 12 S., R. 15 W., and the Brungardt well is in SE sec. 25, T. 12 S., R. 17 W. (Figure 1). The study area is located in the part of the Cretaceous outcrop belt known as the dissected high plains (Merriam, 1963). Current research projects at the KGS are focusing on the channel sands located at the base of the Dakota Formation in Russell County. The test wells were drilled to add shallow well-log and core information to the existing data base.

Three seismic lines were shot near the Haberer well. The sites for the lines were at different stratigraphic levels above the Dakota Formation. Near-surface site conditions varied at each site. A fourth line was shot next to the Brungardt well in Ellis County.

GEOLOGY

Stratigraphy

The Lower Cretaceous rocks in western Kansas comprise the Dakota Formation, Kiowa Shale, and Cheyenne Sandstone (Figure 2). The lower contact of the Cheyenne Sandstone is a major unconformity between Lower Cretaceous rocks and the Lower Permian Nippewalla Group. Above the Dakota Formation is the Upper Cretaceous Colorado Group.

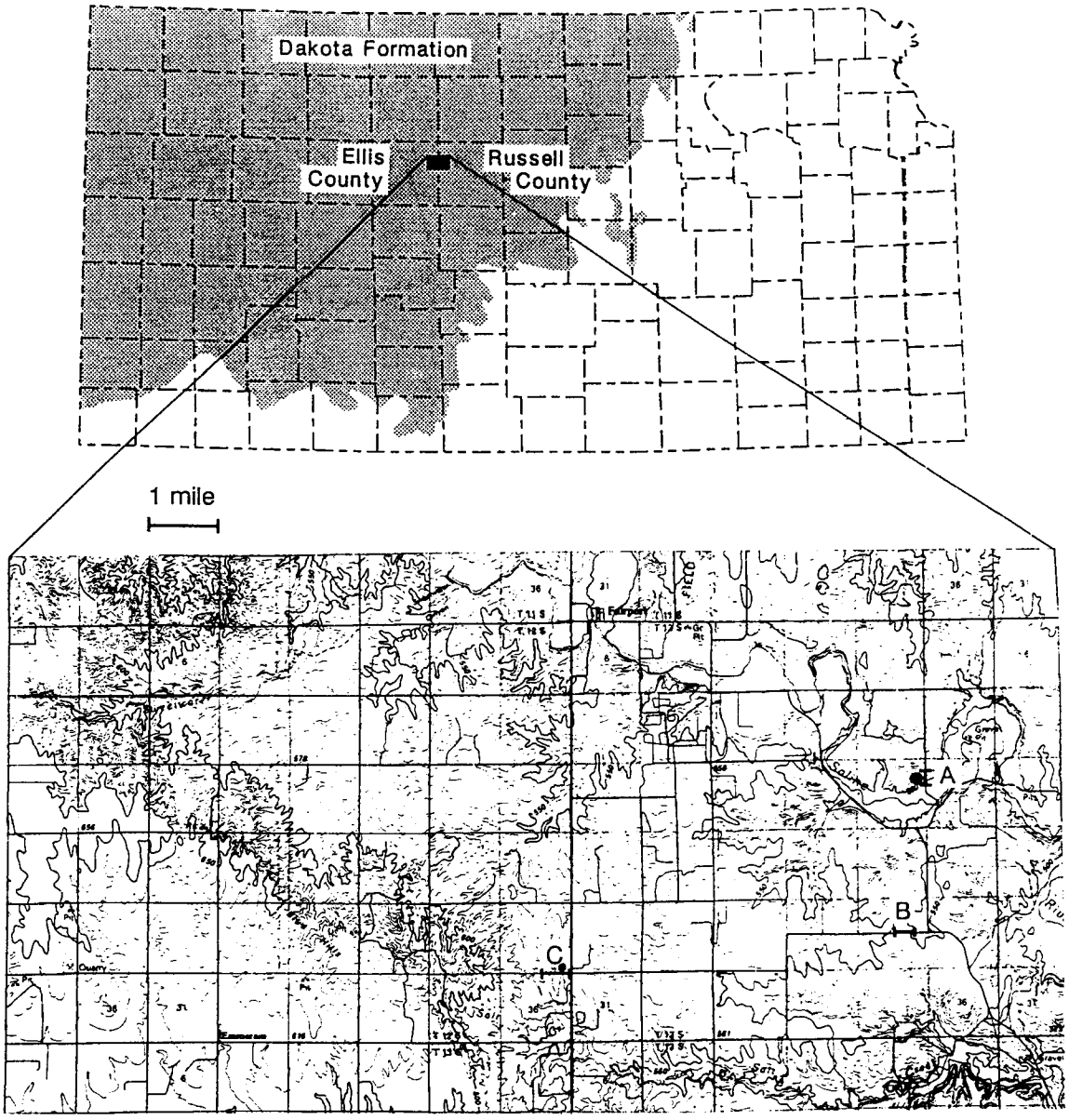

Figure 1. Location of study area. a) Haberer well, line 1, and line 3. b) Line 2. c) Brungardt well and line 4.

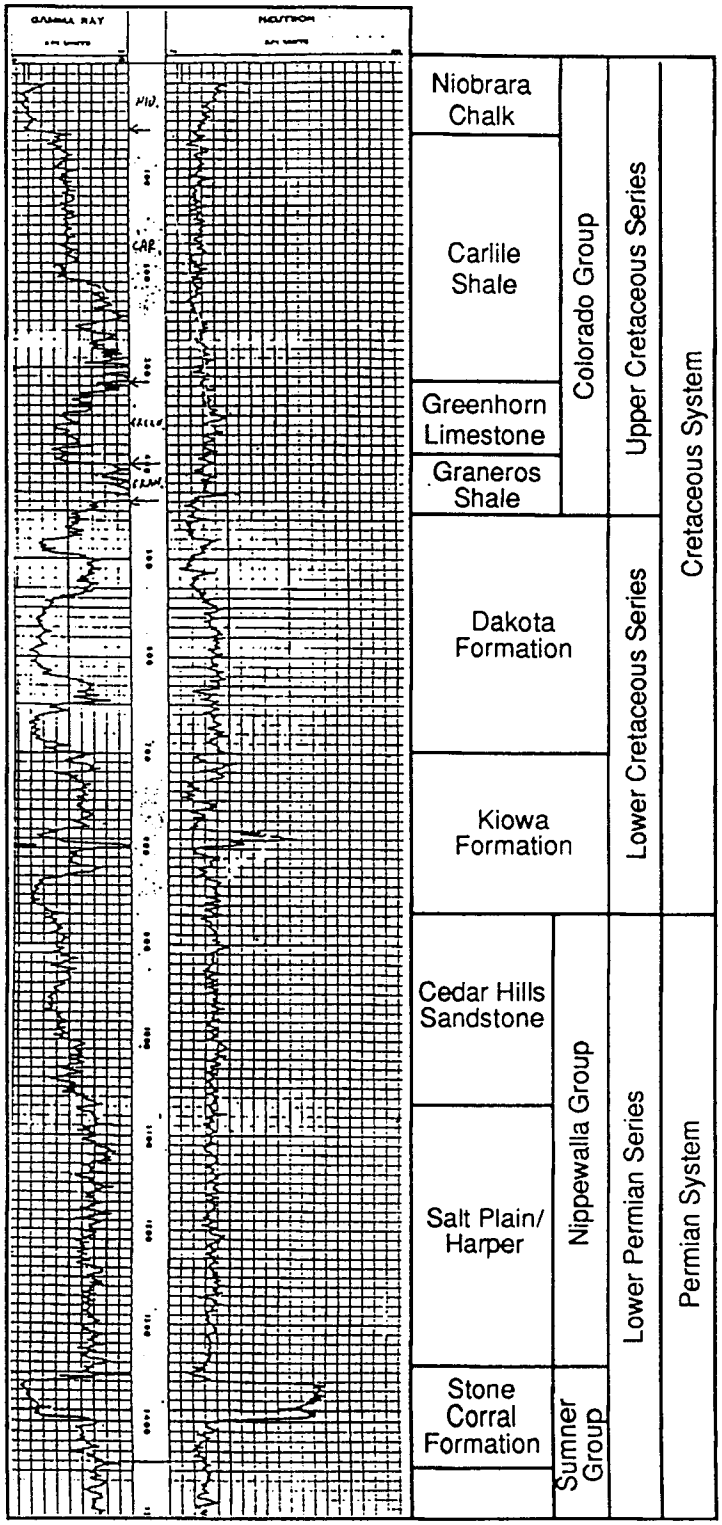

Figure 2. Generalized Stratigraphy in the Study Area.

The Permian Stone Corral Formation is the lowest stratigraphic unit of interest in this study. Depth to the Stone Corral Formation is approximately 215 m at the Haberer well and 385 m at the Brungardt well. The thickness of the Stone Corral Formation is approximately 12.5 m throughout the area. In the subsurface, the Stone Corral Formation consists largely of white to light-gray crystalline anhydrite, commonly referred to as the Cimarron anhydrite. The wide distribution, distinctive lithology, and relatively young age of the Stone Corral Formation have made it a key marker bed in western Kansas. In addition to being easily recognizable on well logs, the Stone Corral Formation produces strong reflections on seismograms (Merriam, 1955). In the Symposium on Geophysics in Kansas, published in 1959, seven out of ten articles on reflection seismic exploration discussed the use of the Stone Corral anhydrite as a reference datum for the computation of reflection time intervals. Changes in the interval time between the Stone Corral Formation and deeper units are considered to be reliable indicators of deeper structure (Beebe, 1959; Care et al., 1959; Rupnik, 1959; Winchell, 1959).

The Salt Plain Formation and the Cedar Hills Sandstone (Permian) of the Nippewalla Group are generally recognized as the only Paleozoic formations above the Stone Corral in the study area (Don Butcher, personal communication 1989). The Salt Plain Formation is composed chiefly of red silty shale (Zeller, 1968). It lies directly on the Stone Corral Formation and is approximately 90 m thick in the study area. Above the Salt Plain Formation, the Cedar Hills Sandstone marks the top of the Permian, and its upper contact represents a major unconformity between the Permian and the Cretaceous.

West of the study area, the unconformity is clearly identifiable using Th/K ratios acquired by spectral gamma ray logging. An abrupt shift is

detected as the tool passes from the Cedar Hills Sandstone, which is rich in feldspar, to the Cheyenne Sandstone, which does not have a high feldspar content (Macfarlane and Doveton, 1989). The unconformity is not as sharply defined on gamma-ray logs.

Although sandstone lenses in the Dakota Formation are the primary subject of this thesis, recognition of sandstone lenses in the Cedar Hills Sandstone would also be useful. Disposal of oil field brine into the Cedar Hills Sandstone can affect the salinity of the Lower Cretaceous aquifers dealt in the study area. Any ability to ascertain the interconnection of the sandstones surrounding the Dakota Formation will aid in predicting possible contamination points.

The Cheyenne Sandstone is not present in the study area. Southeast of the study area the Cheyenne Sandstone is separated from the underlying Permian rocks by a transgressive unconformity that shows a progressive overlapping of Lower Cretaceous rocks on older strata to the northeast (Franks, 1975).

The Kiowa Shale rests unconformably on Permian sandstones in the study area. The sandstone at the base of the Kiowa Shale in the study area is called the Longford Member (Franks, 1975). It is the last unit logged in the Haberer well. The Kiowa Shale above the Longford Member is 5.5 m thick and has a sharp upper contact with the Dakota Formation. In the Brungardt well the Kiowa Shale is 50 m thick (Figure 3).

The Dakota Formation was subdivided into two members by Plummer and Romary (1942): the Terra Cotta Clay Member and the overlying Janssen Clay Member. The Terra Cotta Clay Member is the stratigraphic unit of interest in this study. It is characterized by a mottled light-gray and red kaolinitic clay. Clays were deposited as overbank

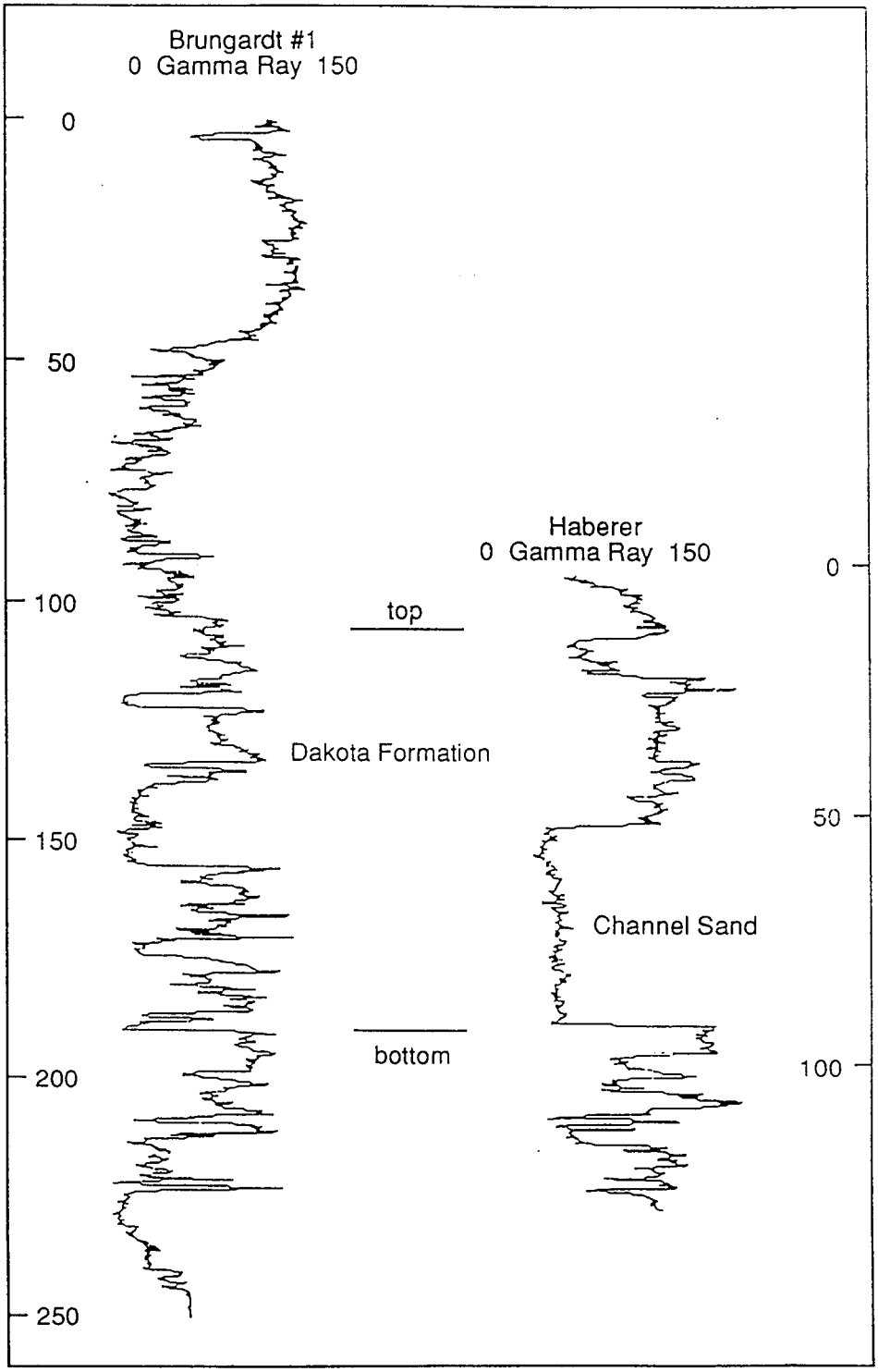

Figure 3. Correlation of the two test wells.

deposits of Dakota streams. The meandering streams left broad lenses of sandstone throughout most of the Terra Cotta clay (Franks, 1975). One such channel has been mapped in the study area (Figure 4).

The channel sand is 41 m thick and lies at a depth of 51 m in the Haberer well (Figure 3). It is absent in the Brungardt well but there are several thin sands (1-3 m thick) at the same stratigraphic position (Figure 3). A sand body 16 m thick is present at a stratigraphic position higher than the channel sand. The total thickness of the Dakota Formation is 84 m in both wells.

The Graneros Shale conformably overlies the Dakota Formation and records the eastward transgression of the shallow Western Interior Sea during the Greenhorn cyclothem. The predominant lithology of the Graneros is noncalcareous silty shale (Hattin, 1965). In the Haberer well the Graneros Shale is overlain by 3 meters of Pleistocene alluvium and is 6 m thick. In the Brungardt well, the Graneros is 11.5 m thick.

The Greenhorn Limestone consists of thin-bedded chalky limestone and calcareous shale (Zeller, 1968). Greenhorn sediments are not penetrated by the Haberer well, which is located just east of the Greenhorn Limestone outcrop belt. In the Brungardt well the Greenhorn limestone is 27 m thick. The top of the Greenhorn Limestone can be recognized in the field area by the outcrop of the resistant Fence-post limestone bed.

The Carlile Shale overlies the Greenhorn Limestone and is present 6 m below the surface to a depth of 65 m in the Brungardt well. The Blue Hill Shale Member is the first member of the Carlile Shale below the surface; it is a fossiliferous, clayey, noncalcareous shale. The underlying Fairport Chalk Member is a fossiliferous chalky shale that contains stringers of

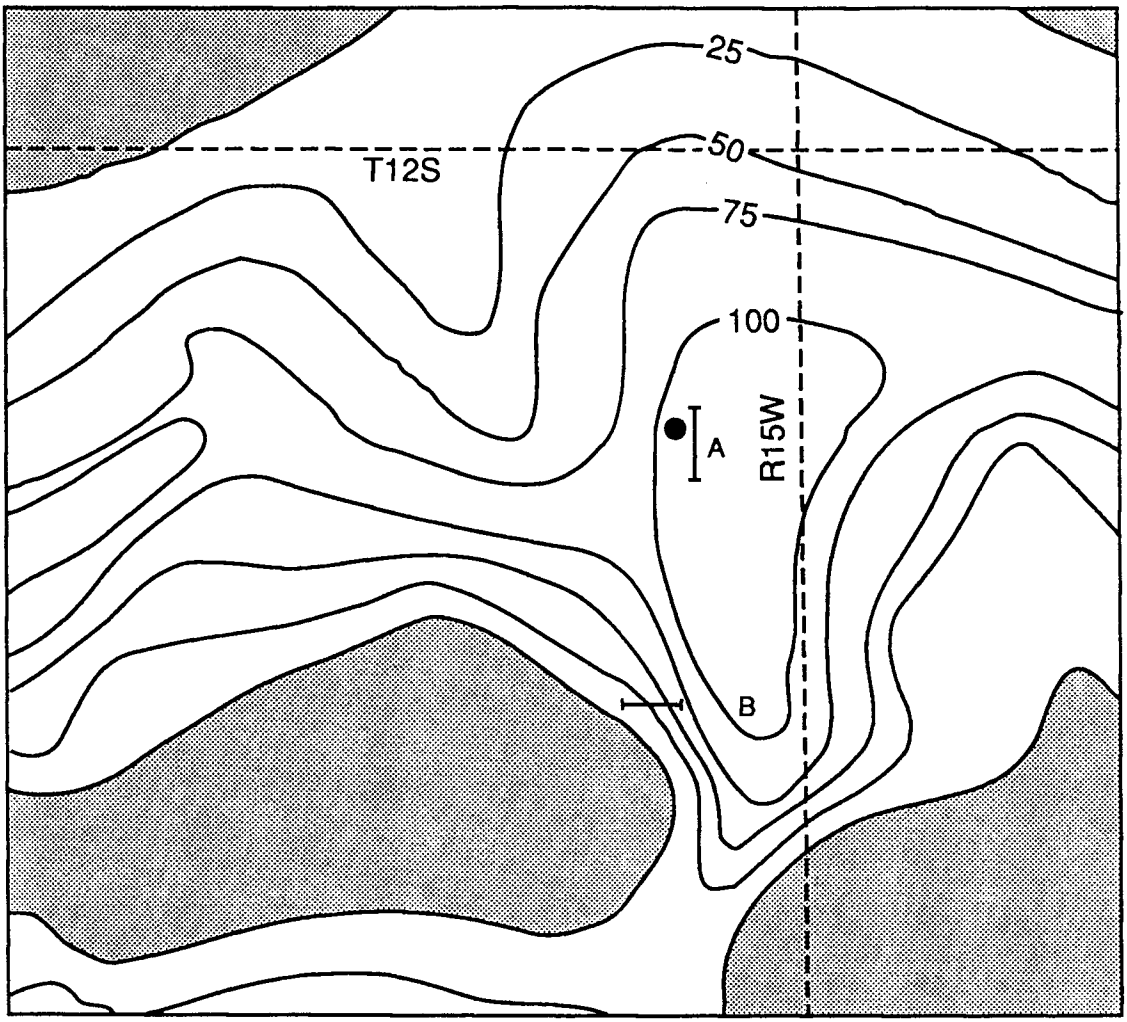

contour interval = 25 feet
channel sand present
channel sand absent
Haberer well
A line 1 and 3 (south to north respectively)
B line 2

Figure 4. Isopach map of the channel sandstone at the base of the Dakota formation (modified from Macfarlane, 1988)

limestone (Merriam, 1963). Above the Carlile Shale there is approximately 6 m of Quaternary sediment at the Brungardt site.

Structure

The Central Kansas uplift is the most prominent structural feature in the study area. It is a northwest-trending structural high that separates the Hugoton embayment to the west from the Salina and Sedgwick basins to the east (Merriam, 1963). A regional structure map contoured on the top of the Stone Corral Formation shows the pre-Desmoinian, post-Mississippian structure as a broad, northwest-sloping surface with no regional arching (Merriam, 1963). The structural dip of the Stone Corral Formation in the vicinity of the Haberer well is less than 1 m/km. This is less than 0.5 m over a distance from line 1 to line 2 on the Stone Corral Formation. The Stone Corral Formation can be considered a flat lying datum on the scale of this study.

RESOLUTION

Temporal and spatial resolution of seismic data are interrelated. Improving one automatically improves the other (Lindsey, 1989). They both depend on wavelength. The dominant wavelength (λ) is determined by the velocity (v) and the dominant frequency (f) of the seismic wave.

$$\lambda = v/f$$

The only variable affecting wavelength that can be controlled during acquisition is frequency. High frequency data will allow greater resolution.

Temporal or vertical resolution in exploration seismology involves the ability to distinguish that more than one interface is involved in a reflection. The resolvable limit which is the minimum separation that two interfaces can have and still be recognized, is dependent on the background noise and the interpreters' ability to see minor changes in waveshape (Sheriff, 1977). The Rayleigh resolution limit, which is 1/4 of the dominant wavelength, is the generally accepted limit on vertical resolution (Widess, 1973; Sheriff, 1984; Yilmaz, 1987). Put another way, the thinnest bed for which a distinct reflection can be seen from both the top and bottom of the bed is 1/4 of the wavelength.

Spatial or lateral resolution refers to how close two reflecting events can be situated horizontally, yet be recognized as two separate points rather than one (Yilmaz, 1987). The limit of spatial resolution is determined by the width of the first Fresnel zone. The first Fresnel zone is the reflector area in which reflected energy arrives at the receivers within a half-cycle so that interference is constructive (Sheriff, 1985). The radius of the Fresnel zone (r) depends on wavelength (λ) and reflector depth (z).

$$r = (z\lambda/2)^{1/2}$$

This equation can also be written in terms of frequency (f), velocity (v), and two-way travel time (t) (Knapp and Steeples, 1986).

$$r = (v/2)(t/f)^{1/2}$$

A decrease in wavelength or the related increase in frequency will decrease the radius of the Fresnel zone and increase the spatial resolution of the data.

Obtaining high resolution data was the goal of this study. Source, receivers, and line parameters were all chosen to increase the frequency of the data recorded. The data recorded had dominant frequencies ranging from 95 Hz to 200 Hz. With an average formation velocity of 2500 m/s, the vertical resolution ranged from 6.6 m to 3.1 m. Resolution of the data to these limits depended heavily on the amount of noise present on the seismic record. The spatial resolution ranged from 17 m to 25 m at a depth of 50 m and from 49 m to 71 m at a depth of 385 m. These are the depths from the top of the channel sand in the Haberer well and the top of the Stone Corral Formation at the Brundgardt well, respectively.

DATA ACQUISITION

Equipment and Instrumentation

A downhole .50 caliber rifle (Figure 5) was used as an energy source to collect low-cost shallow seismic reflection data. The downhole rifle was used because it has a higher frequency source pulse and an increased signal-to-noise ratio compared to the silenced surface .50 caliber rifle used in previous work (Steeples et al., 1987).

One 750-grain bullet was fired at each shot location. A hole approximately 1 m deep was drilled at each shot location previous to using the downhole rifle.

A Giddings auger towed by a field vehicle was used to drill shot holes. It worked well when shot holes were located on roads or in level

Downhole .50 cal. rifle

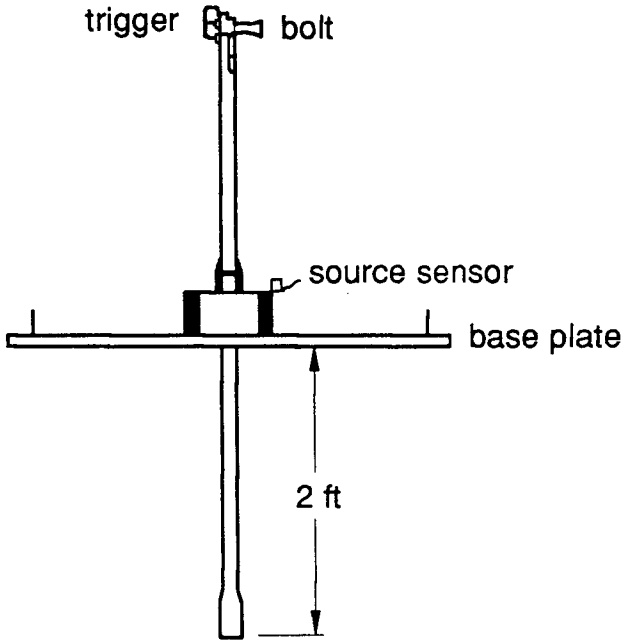

Figure 5. To operate, two graduate students stand on the base plate and fire the rifle.

fields. Shot holes were also drilled using the Terrapro, a recently developed auger-equipped fourwheeled vehicle (see Appendix A).

The seismic recording truck is equipped with an Input/Output DHR 2400 seismograph. It is a 24-channel fixed-gain system with an 11-bit analog-to-digital (A/D) converter plus 1 sign bit. Modules having switch selectable 55-110-220 Hz and 110-220-340 Hz low-cut filters were used in the DHR 2400 during recording. The filters have 24-dB/octave rolloff below their corner frequencies. The 220-Hz low-cut filter reduces the amplitude of 110-Hz energy by 24 dB and 55-Hz energy by 48 dB before A/D conversion. Lowcut filters were used before A/D conversion to cut down the magnitude of low-frequency components. This allowed a significant number of bits to be filled with high-frequency signal (Knapp and Steeples, 1986). High-cut filters were used to reduce the amplitude of unwanted high-frequency noise and to prevent aliasing of high frequencies. The seismograph has 3000-Hz (-60 dB point) anti-alias filters that are always in use. Analog gains were used to amplify the seismic signal close to but not greater than the maximum voltage accepted by the A/D converter.

Receiver groups were composed of two series-connected 100-Hz geophones on line 1 and three series-connected 40-Hz geophones on lines 2, 3, and 4. High-frequency geophones acted as an additional low-cut filter because they had a -6-dB/octave response to frequencies below their resonant frequency (Knapp and Steeples, 1986). The series-connected geophones were planted in short arrays either in line, to help cancel the air-coupled wave generated by the source, or perpendicular to the line, to cancel wind noise. Aside from cancelling horizontally traveling noise, series-connected geophones added vertically arriving signals in phase.

Walkaway Noise Test

Acquisition parameters chosen for a shallow seismic survey control the quality, resolution, and ability to record reflections from a particular horizon. The optimum window technique has been used successfully to record shallow reflectors from bedrock using common offset techniques (Hunter et. al., 1984). At the KGS, similar techniques combined with common depth point (CDP) acquisition and processing have provided a technique to gather reflection information for a variety of shallow engineering, structural, groundwater, and environmental projects (Steeples and Miller, 1988; Myers et al., 1987; Treadway et al., 1987). Before going in the field, simple modeling of the expected target is used to help select acquisition parameters. Once in the field, a walkaway test is used to check and improve the selection of parameters (Knapp and Steeples, 1986).

Walkaway noise tests were used to determine acquisition parameters at each of the sites in this study. The procedure was as follows: Forty-eight or more closely spaced receiver locations were laid out with the geophones in each group planted next to each other (bunched). The source was placed at one receiver location spacing from the end of the line then moved away from the line. Shots were taken at increased intervals, providing a continuous record of seismic response at changing source-receiver offsets. Filter and gain settings were adjusted with each shot. Field plots of each of the seismic records were then analyzed to determine receiver spacing, shot spacing, source to near receiver offset, maximum receiver offset, high-cut and low-cut filters, notch filter, gains, and sample interval for each of the four lines collected for this study (see Appendix B). All the lines were shot using end-on spread geometry (Figure 6).

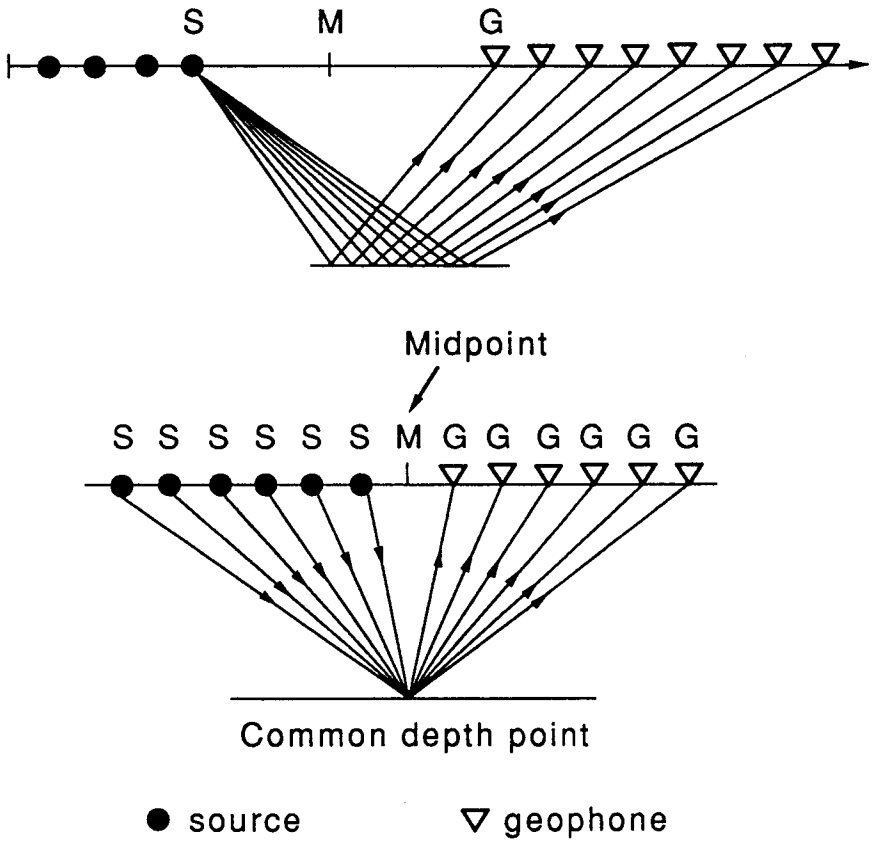

Figure 6. (a) All the data was shot using end-on geometry.
(b) Data was then sorted into CDP gathers during processing.

Topography

During data acquisition, it is necessary to accurately describe the line geometry and any deviations from that geometry. Any changes in the position of the receiver or of the shot locations from the normal geometry can be accounted for during processing. One important change along the line that needs to be described is elevation. An elevation change at the surface might be interpreted as dip on the reflector if it was erroneously assumed that the surface was flat.

A hand-level and stadia rod were used to measure relative elevation changes every fifth station along line 2 and line 3 (Figure 7). Line 1 and Line 4 were relatively flat and elevations were not measured.

DATA PROCESSING

All the data collected for this study were processed on the Data General MV-20000 computer at the KGS. The Seismic Processing Executive software (SPEX) marketed by the Sytech Corporation was used for all processing procedures except F-K filtering.

The goals of processing were to improve the signal-to-noise (S/N) ratio of the data and to display the data as stacked CDP seismic sections convenient for geologic interpretation. The amount of signal recorded in the field cannot be increased by data processing. Processing is used to remove, or at least suppress, noise. In this way, the S/N ratio can be increased and reflections can be more easily identified.

The general processing flow used is shown on Table 1. For a general explanation of these processes, see Yilmaz (1987). Static corrections and F-K filtering are discussed further.

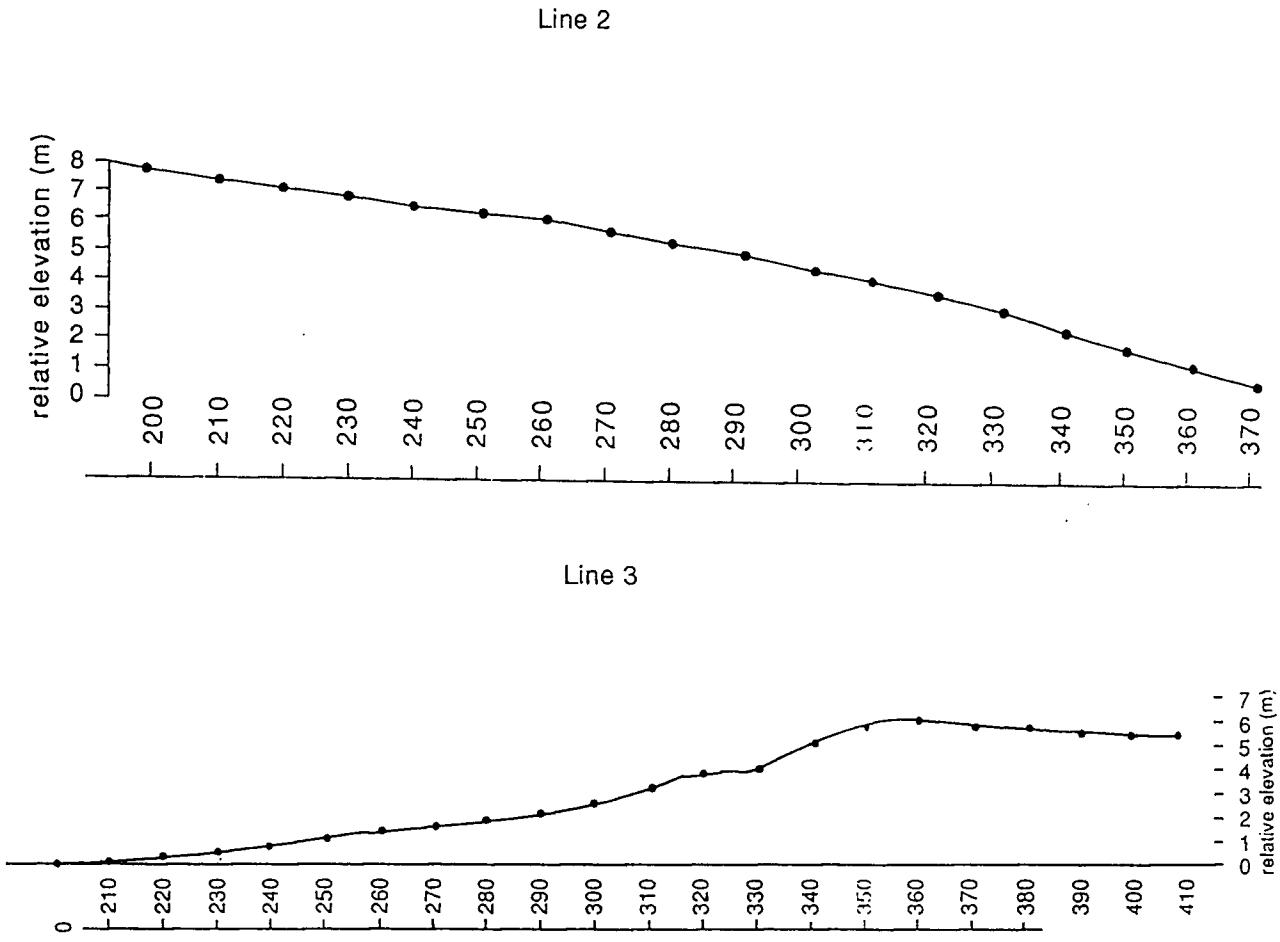

Figure 7. Relative elevation on line 2 and line 3.

TABLE 1

General Processing Flow

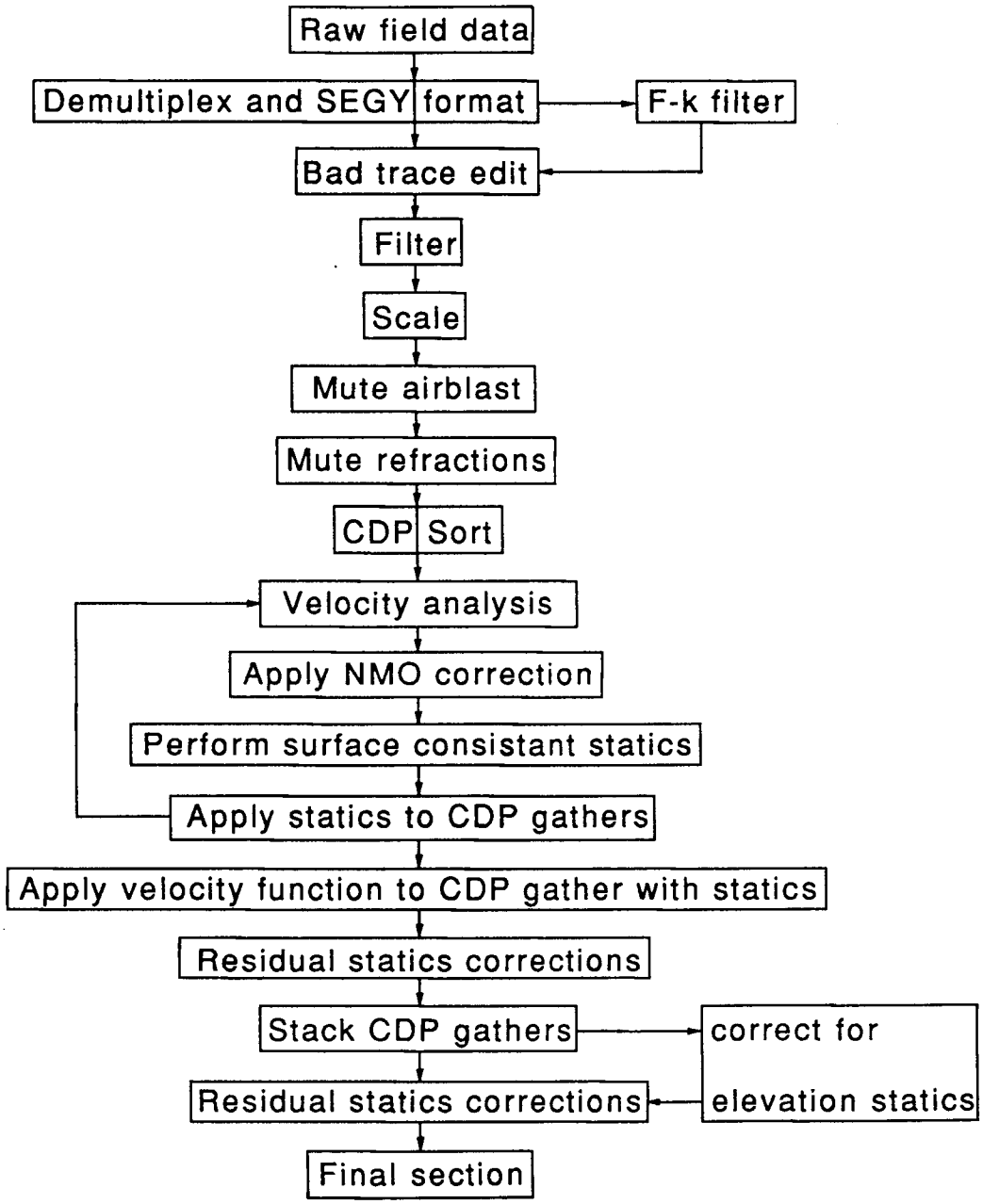

Static Corrections

If the near-surface material on each line has a constant seismic velocity, then the calculation of the elevation static correction is trivial. All that is required is to simply add or subtract the amount of time required for the seismic energy to travel the vertical distance between a reference elevation and the elevation measured (Dobrin, 1976). Velocity variations in the near surface, however, vary laterally along the lines, with depth, and with elevation. These variations make static corrections for elevation difficult. Minor variations in travel times associated with minor depth changes of the near surface and with small elevation differences can be accounted for using AUTS, an automatic statics process available in SPEX, which computes a series of surface-consistent statics. This process cannot correct for changes in elevation across the whole line. At this point the data can be interpreted so long as the change in elevation is taken into account (Figure 8). For this study a correction for topography was not necessary to interpret the data. However, the Stone Corral Formation was be used to make elevation corrections by picking a reference time closest to a control point. The amount of time shift necessary to move the Stone Corral reflection to the reference time was measured off the final stacked section. The time shifts were applied using the Statics Application card (STAT) available in SPEX. After the shift was applied, residual statics were applied to correct for minor errors in the time shift calculation (Figure 9).

F-K filtering

One of the problems with shallow reflection seismology is coherent linear noise (air-coupled waves, ground roll, refractions, and direct arrivals), which obscures reflection information arriving at the same time.

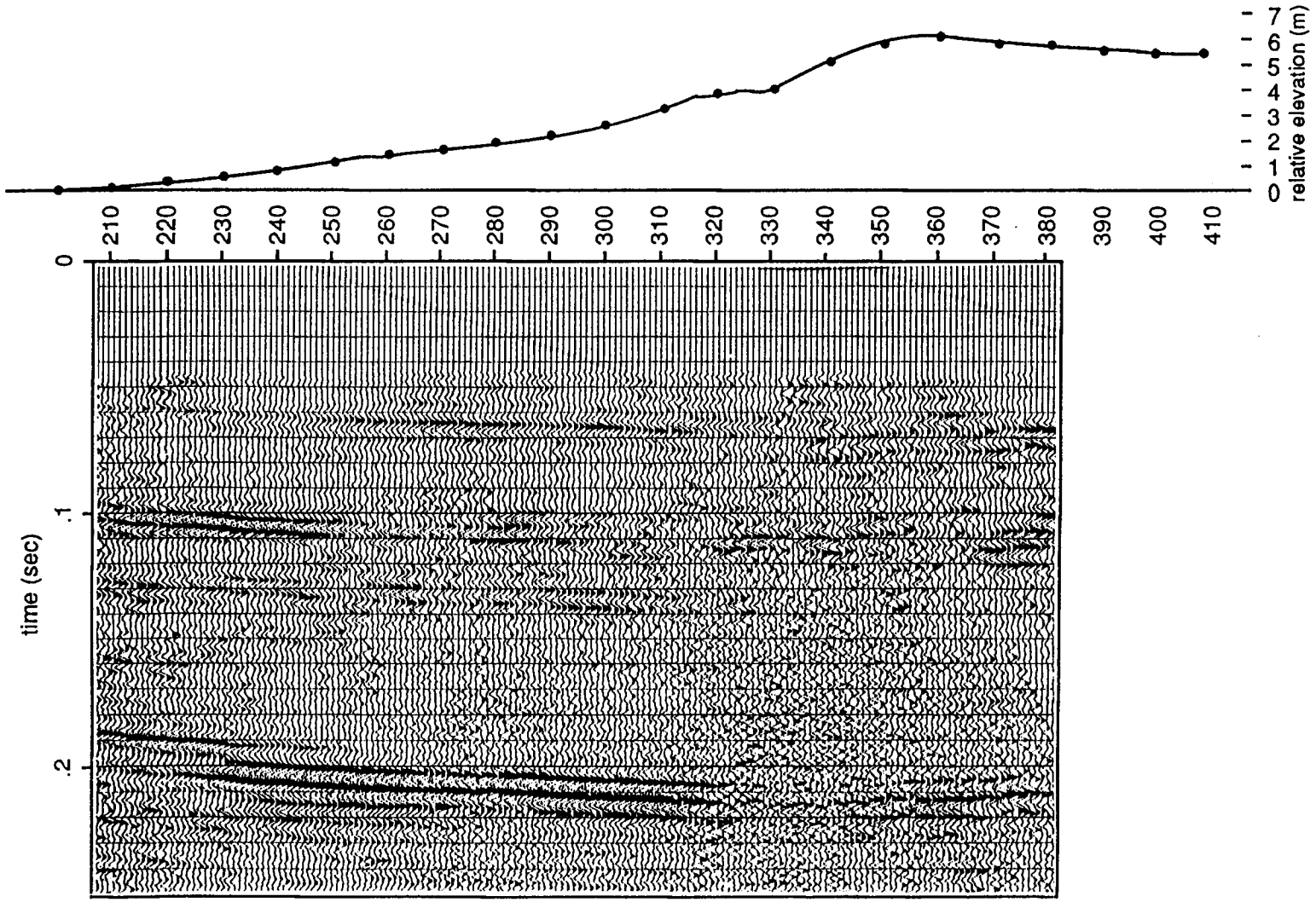

Figure 8. Reflectors dip to the north due to the change in topography.

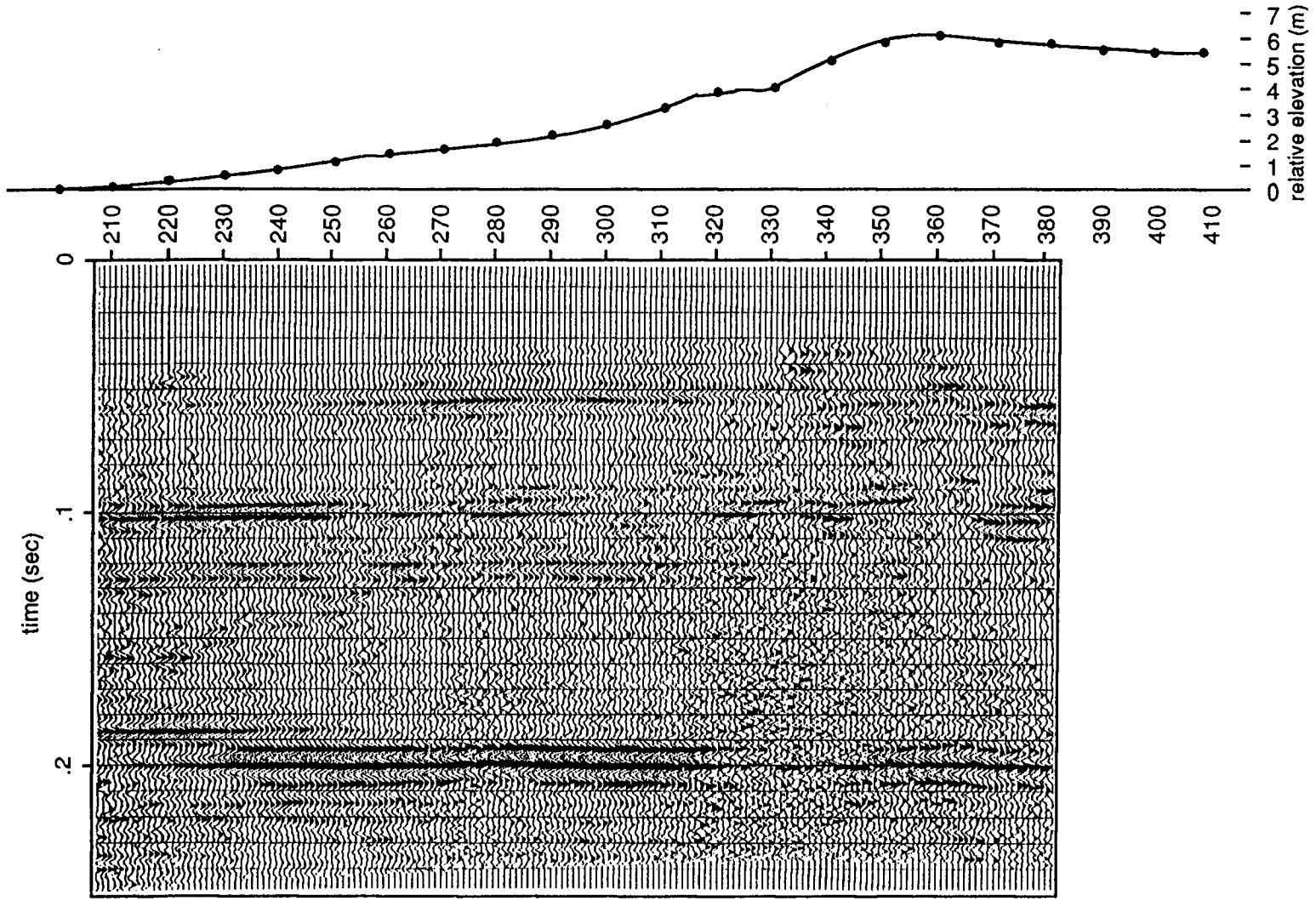

Figure 9. Elevation static correction are applied that flatten the Stone Corral reflection at 2 seconds.

Frequency filtering can be used to suppress noise when the noise and signal have different frequencies. The noise and signal, however, often have similar frequencies and cannot be discriminated by frequency filtering. This is when F-K filtering is extremely useful.

Dipping events in the time-space (t-x) plane can be separated by their dips in the frequency-wavenumber (f-k) plane. In f-k space, the coherent linear noise can be isolated from reflection energy and then eliminated (Yilmaz, 1987). A two-dimensional Fourier transform is used to transform the data from (t-x) space to (f-k) space (Figure 10). Conventional implementation of the Fourier transform can lead to wraparound noise. Extension of the data beyond the ranges of the spatial and temporal axes, by padding with zeros, can help to avoid this problem. Increasing the size of the array increases the time and cost of the operation (Yilmaz, 1987).

To help eliminate the coherent linear noise seen on line 1 an f-k filtering program was used. The f-k filter was designed to remove energy with a particular velocity. Linear moveout was applied to the data in t-x space at the velocity to be removed. After the data was transformed into f-k space, the unwanted linear noise was aligned vertically along the frequency axis with a wavenumber of zero. The wraparound also lined up on the axis, eliminating the need for excessive padding with zeros. A fan cut filter, centered at a wavenumber of 0, was then applied. The input into the program was the file name, trace spacing and the width of the fan filter. The velocity to be removed was the center of the fan chosen. Because the tapering was very smooth, a wide fan was used. A test of the filter on field files from line 2 shows that it removed linear noise (Figure 11). One important advantage of using linear moveout before applying the two-dimensional Fourier transformation and extremely gentle tapering is that

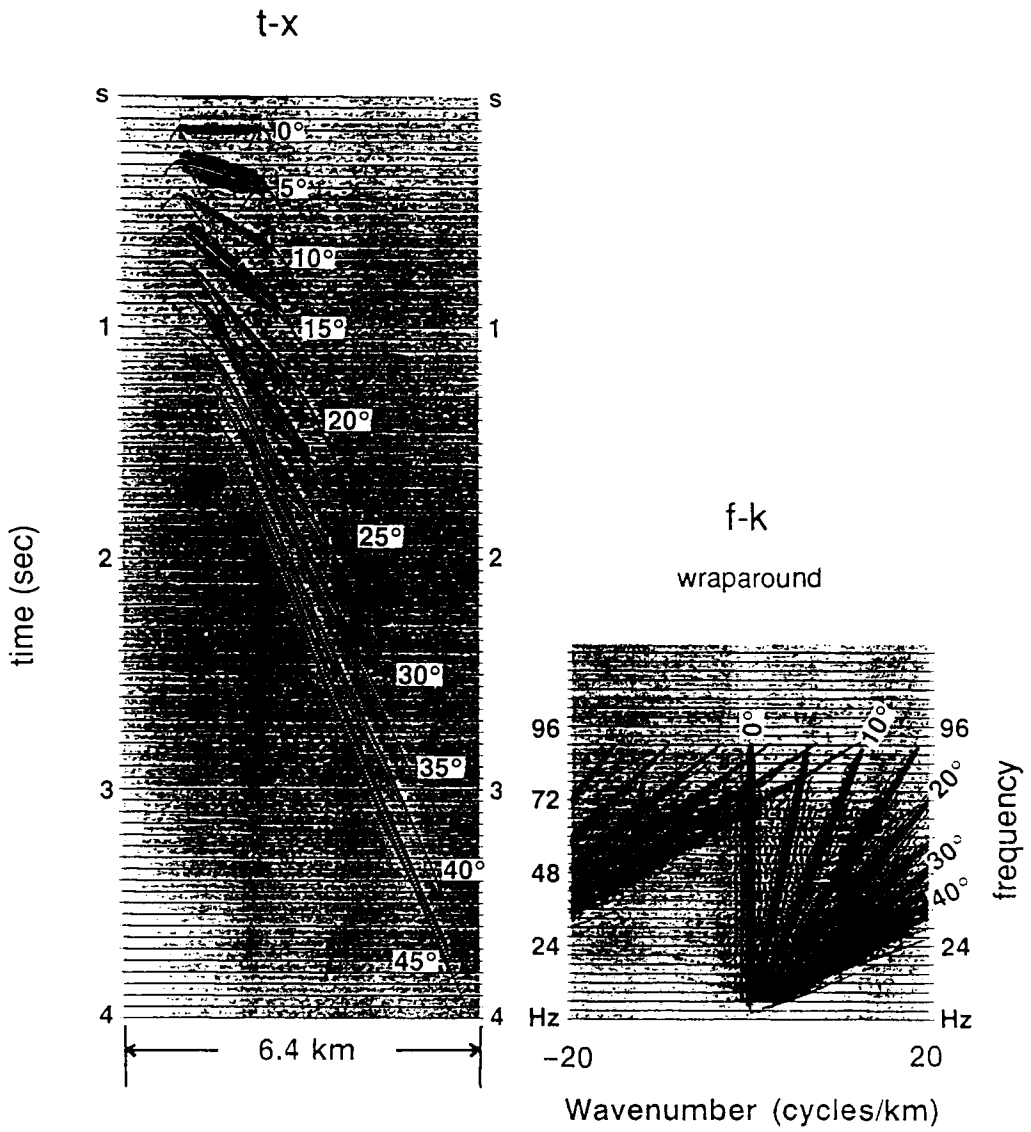

Figure 10. Dipping events on field records are plotted as dipping events in the F-k domain. Horizontal events in t-x space align vertically with the frequency axis at wave number 0 in F-k space.

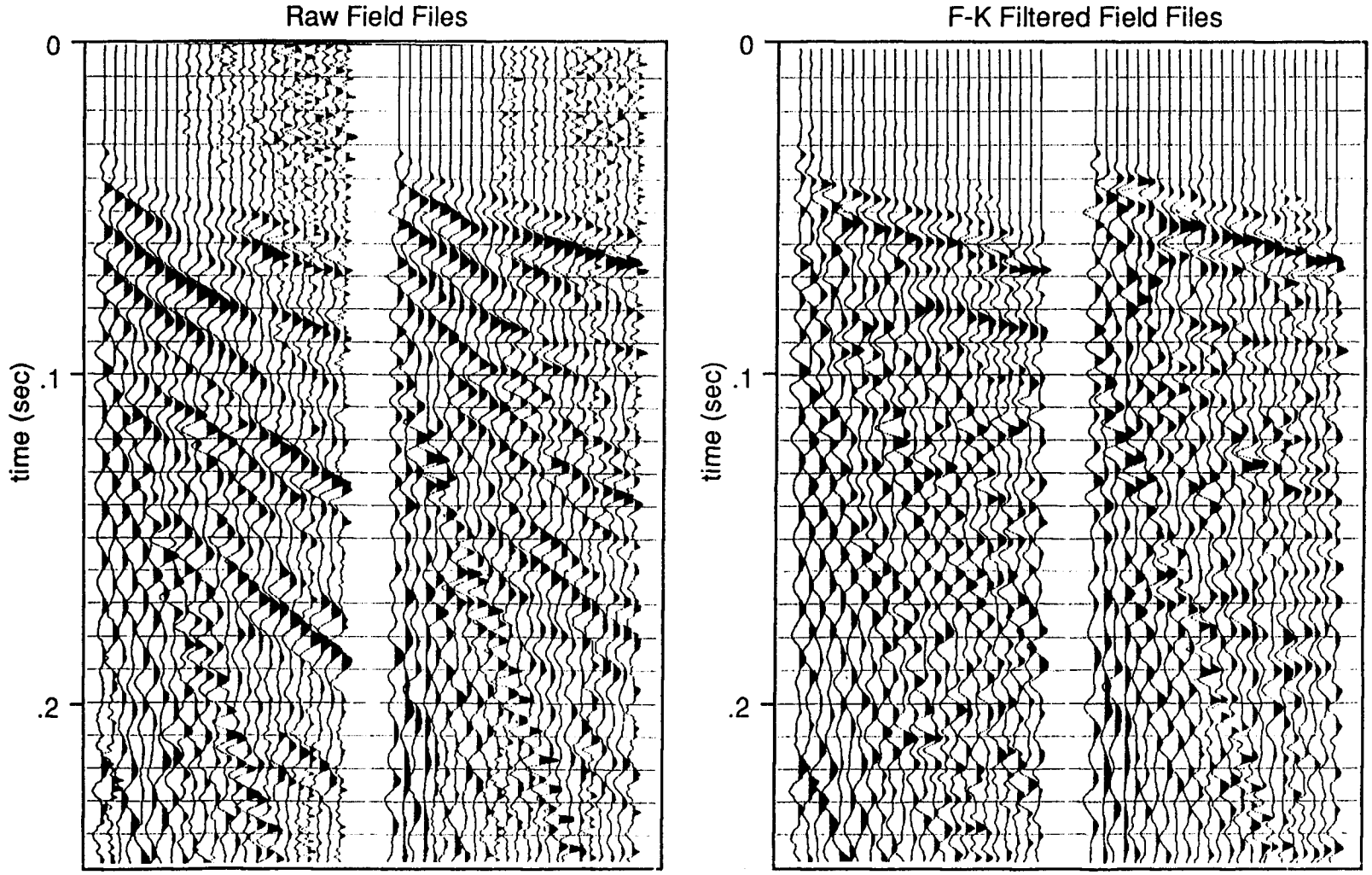

Figure 11. F-k filter was applied twice. Once to to remove linear noise at 1250 m/s and then to remove noise at 1350 m/s.

artifacts that might be misinterpreted as true reflections were not created.

SYNTHETIC SEISMOGRAMS

A synthetic seismogram is an artificial seismic record manufactured by assuming that a waveform travels through an assumed model (Sheriff, 1984). One-dimensional synthetic seismograms are often made using well-log data. They can be used to tie reflecting events on seismic sections to well logs. Thus information about strata known from the well can be extended to undrilled regions through the use of reflection seismology.

The principal logs of interest in making a synthetic seismogram are the sonic or velocity log and density logs. First, the velocity (v) and density (p) values converted from depth to time are multiplied to get the acoustic impedance Z:

$$Z(i) = v(i) \times p(i).$$

The acoustic impedance values are used to calculate the reflection coefficients R with time:

$$R = [Z(i) - Z(i-1)]/[Z(i) + Z(i-1)].$$

The refection coefficients are then convolved with a seismic wavelet to form the seismic trace (Figure 12).

Because the density of sedimentary rocks varies less than their seismic velocities, the reflection coefficient is primarily affected by the

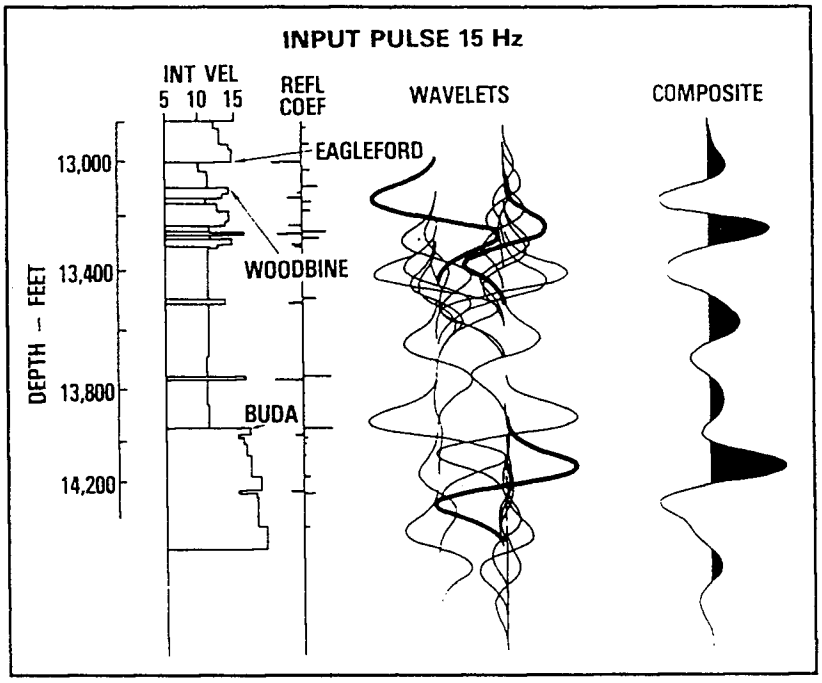

Figure 12. Calculation of a synthetic seismic trace from velocity information (from Vail et al., 1977).

velocity contrast of two sedimentary layers (Telford, 1976). Thus density values can be considered constant and the reflection coefficients are commonly estimated from the values of the sonic or velocity log only using the following equation:

$$R = [v(i) - v(i-1)]/[v(i) + v(i-1)].$$

The synthetic seismograms used in this study were created using the Snark module in TERRALOG (Doveton and Cable, 1980). This program assumes a constant density and calculates reflectivity series based on sonic or pseudo-sonic logs only. Figure 13 shows the output of the Terralog program. Synthetic seismic traces were calculated using a 100-Hz Ricker wavelet and the sonic log from the Brungardt well. The amplitude values created from the program were saved in a disk file using the file command in TERRALOG. Then, using the program TERRATOKGS.PR the synthetic traces were converted to SPEX format. This allowed the synthetic traces to be scaled and plotted using the SPEX package.

Pseudo-sonic Logs

When velocity or sonic logs are not available, it is sometimes possible to make pseudo-sonic logs by calculating empirical relationships between the available types of well logs and velocity. In this study, the logs from the Brungardt well were used to determine a set of coefficients that would relate the gamma ray, density, and neutron porosity log to the sonic log.

Each type of log was plotted against the sonic log to determine whether there were any relationships (Figure 14). The plot of the neutron

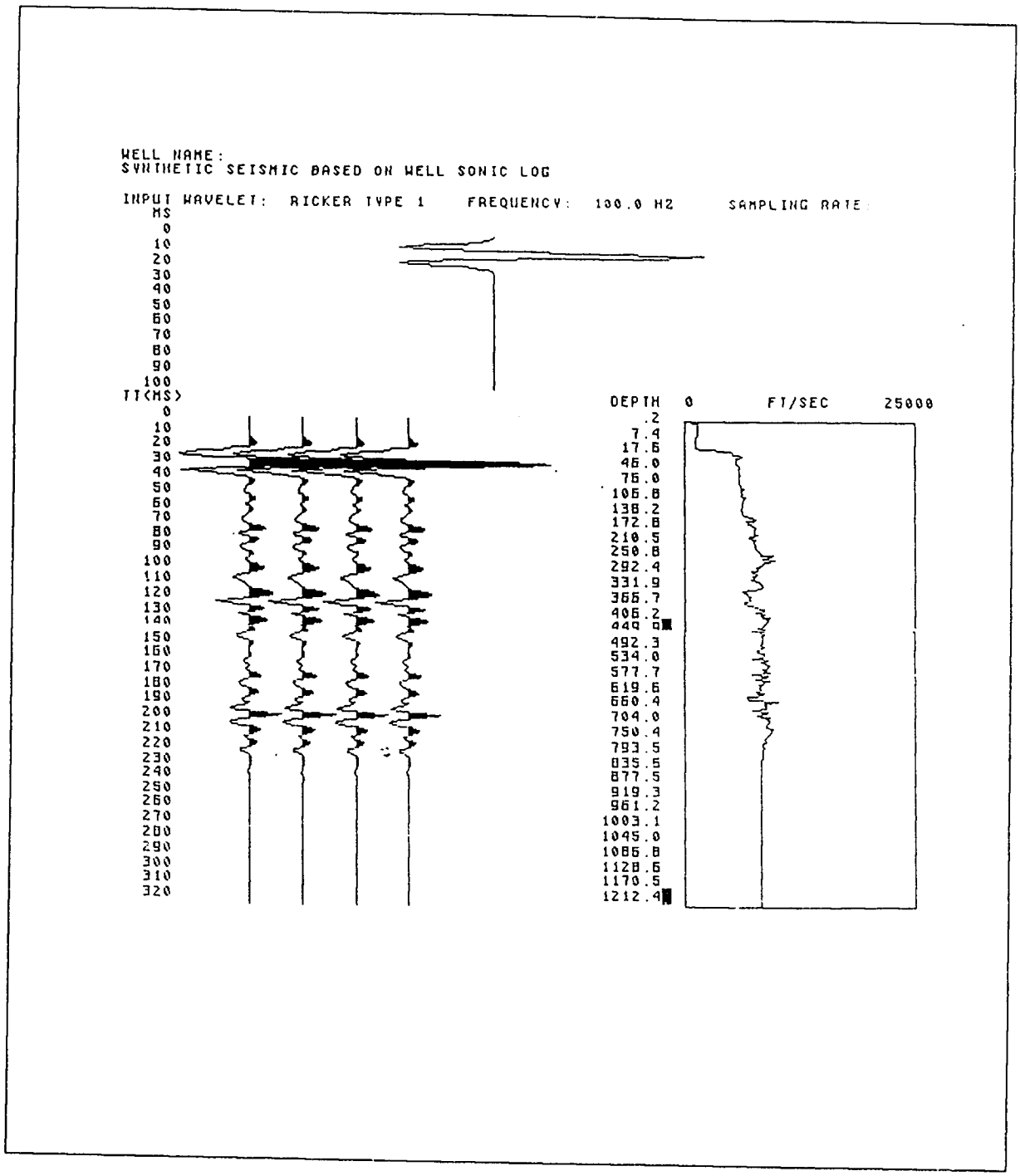

Figure 13. Terralog output using the sonic log from the brungardt well and a 100 Hz Ricker wavelet.

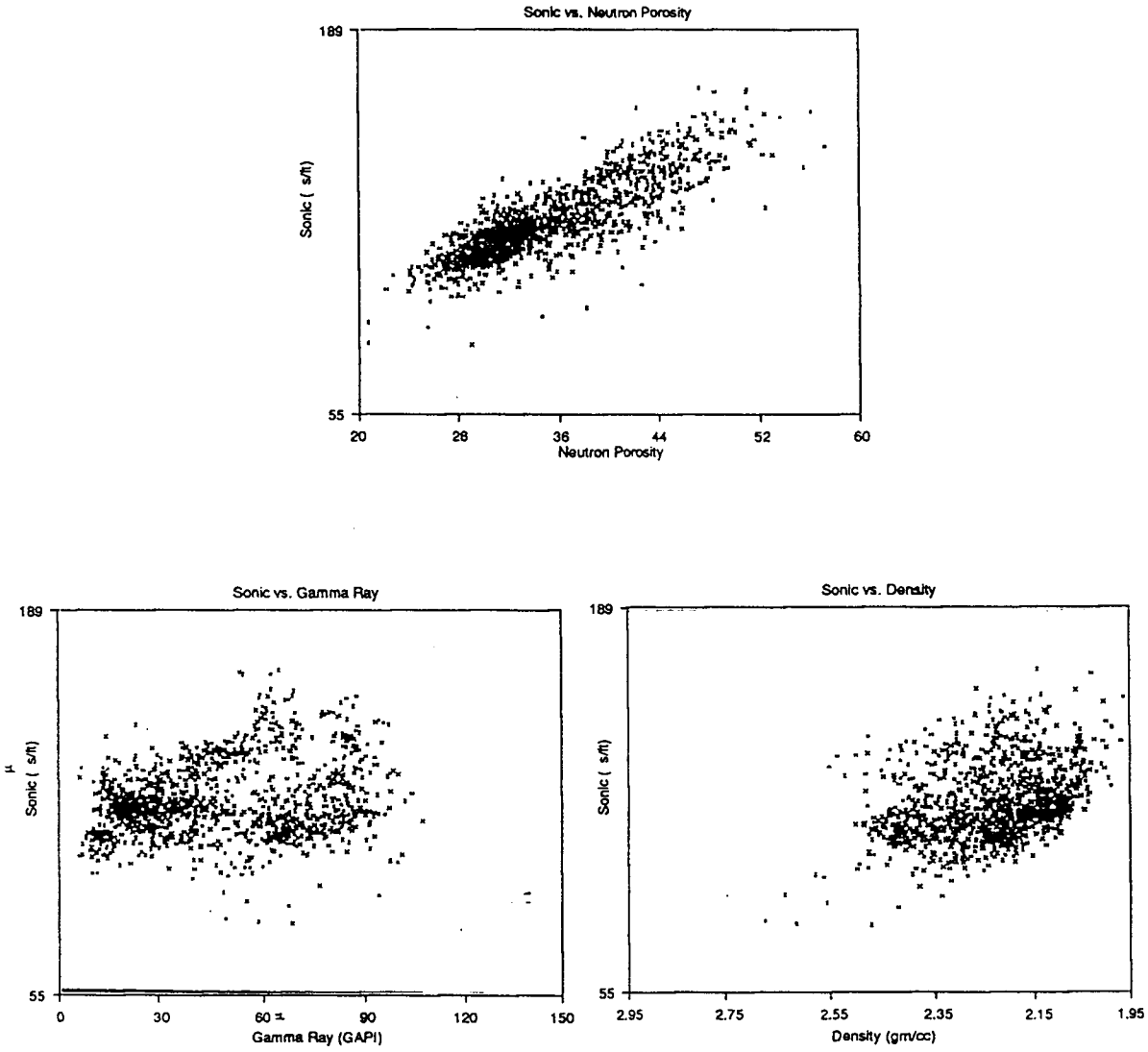

Figure 14. The neutron porosity log shows a linear trend with the sonic log.

porosity values against the sonic values shows a well-defined linear relationship. The gamma ray and litho-density values do not show a direct relationship to sonic values. When the velocity log and the neutron porosity log are plotted together, the correlation between the porosity values and the sonic values is obvious (Figure 15).

The neutron porosity tool measures the amount of hydrogen in a formation. Water, whether in the pore space, bound in clays, or in a crystalline structure such as gypsum, is the primary source of hydrogen being measured. The relationship between the sonic log and porosity log indicates that, as water content increases, velocity decreases. The shales in the interval of interest are only moderately compacted, as seen by their high water content.

Although the neutron porosity (NPOR) log showed the greatest correlation with the sonic log (DT), both the gamma ray (GR) and litho-density (DEN) logs were used to predict sonic values in the Haberer well. Other researchers in Kansas have noted the relationship between neutron porosity values and sonic values and used this information to make pseudo-sonic logs from neutron porosity logs when sonic logs were not available (Ready, 1985; Seeber, 1985). The predictive value of the neutron porosity log is fortunate because neutron porosity logs are commonly run in Kansas wells. In this case the neutron porosity log alone was sufficient to make a pseudo-sonic log but all the information was used because it was readily available.

The following equation was solved for coefficients A, B, C, and D using linear regression on the logs from the Brungardt well:

$$DT = A + (B \times GR) + (C \times DEN) + (D \times NPOR).$$

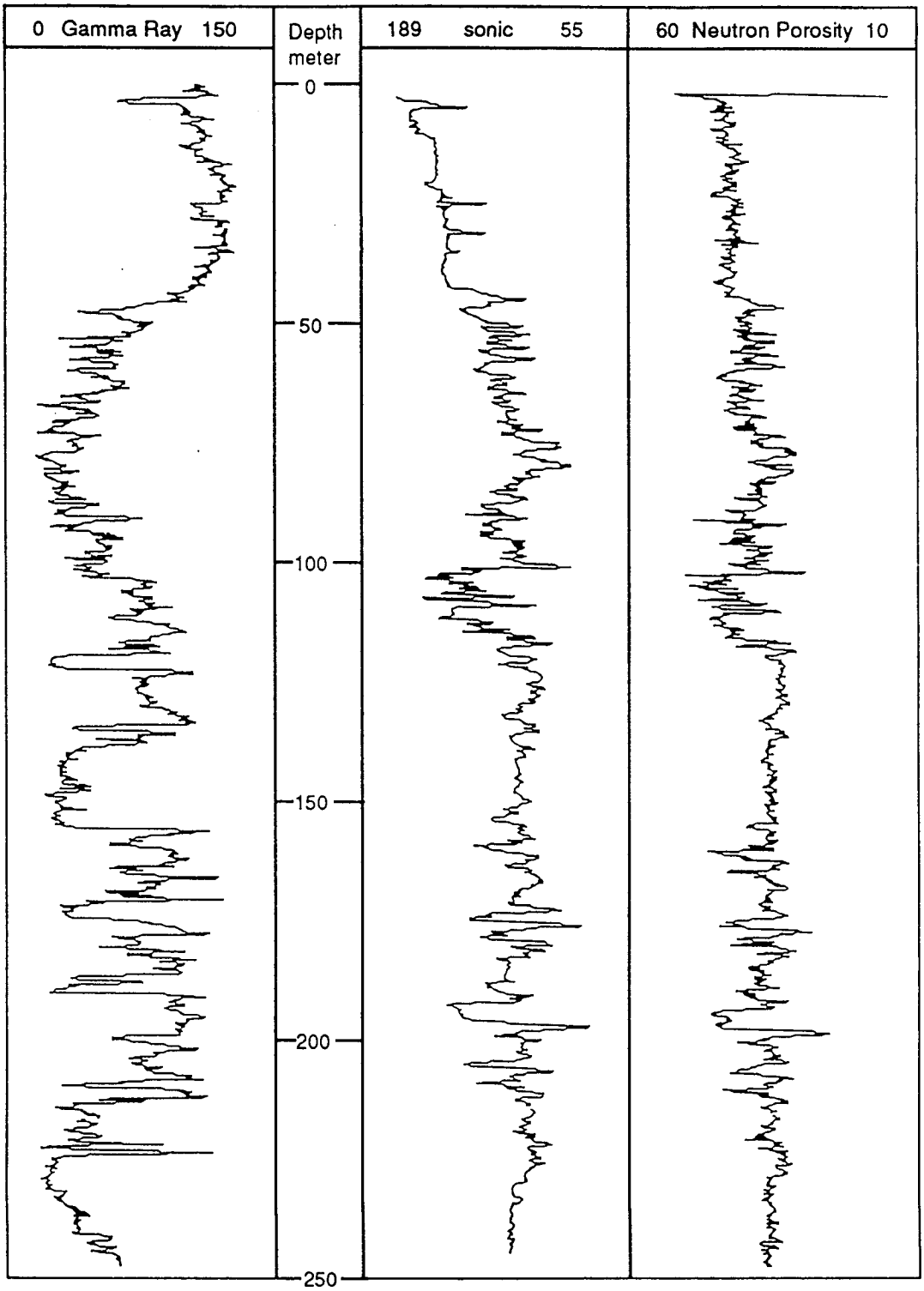

Figure 15. Comparsion of sonic log and Neutron Porosity log,Brungard#1 well. The sonic log and neutron porosity log show strong correlation.

The regression was made using values from a depth of 150 ft (45.7 m) to 800 ft (243.8). The values for coefficients are given in table below.

Table 2. Regression Coefficients.

Depth Interval	A	B	C	D
150-800 ft (46-244 m)	77.183	0.029	-7.425	1.689
350-650 ft (107-198 m)	69.167	- 0.045	-4.304	1.859

A comparison of the synthetic seismic trace made from the sonic log and one made from a pseudo-sonic log using the coefficients found using a linear regression equation shows good correlation (Figure 16). The interval used to calculate the coefficients included the Greenhorn Limestone, which consists mostly of limestone and chalky shale (Merriam, 1963). The Haberer well, where the pseudo-sonic log is needed, does not go through the Greenhorn Limestone. It begins in Pleistocene alluvium just above the Graneros Shale. The Graneros Shale, the Dakota Formation, and the Kiowa Shale are the only units logged in the Haberer well. A second set of coefficients was calculated using the interval from 350 ft (107 m) to 650 ft (198 m) in the Brungardt well, which correlates to the interval penetrated by the Haberer well. The synthetic seismic traces made from the Haberer well logs uses the second set of coefficients in Table 2.

The pseudo-sonic log calculated for the Haberer well is shown in Figure 16, together with the gamma ray log and the neutron porosity log. The strong influence of the neutron porosity log in creating the pseudo-sonic log is obvious. The target sandstone at the base of the Dakota

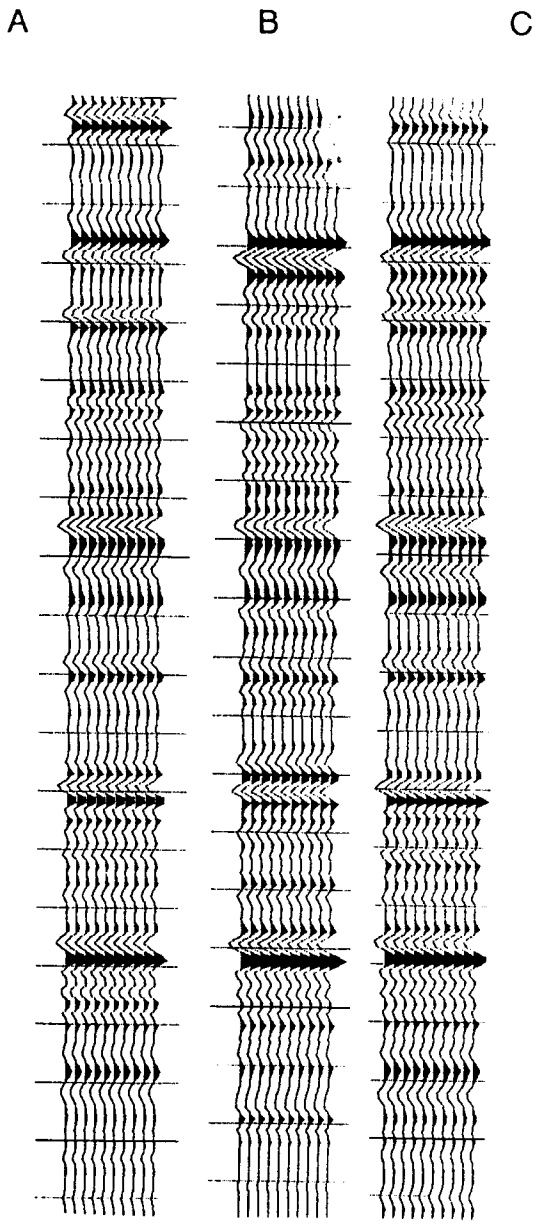

Figure 16. Comparison of synthetic seismograms made from the sonic log in the Brungardt well and pseudo-sonic logs calculated from other well logs. A) pseudo-sonic calculated from neutron porosity log. B) sonic log. C) pseudo-sonic calculated from gamma ray, density, and neutron porosity logs.

Comparsion of pseudo-sonic log and Neutron Porosity log

Haberer Well

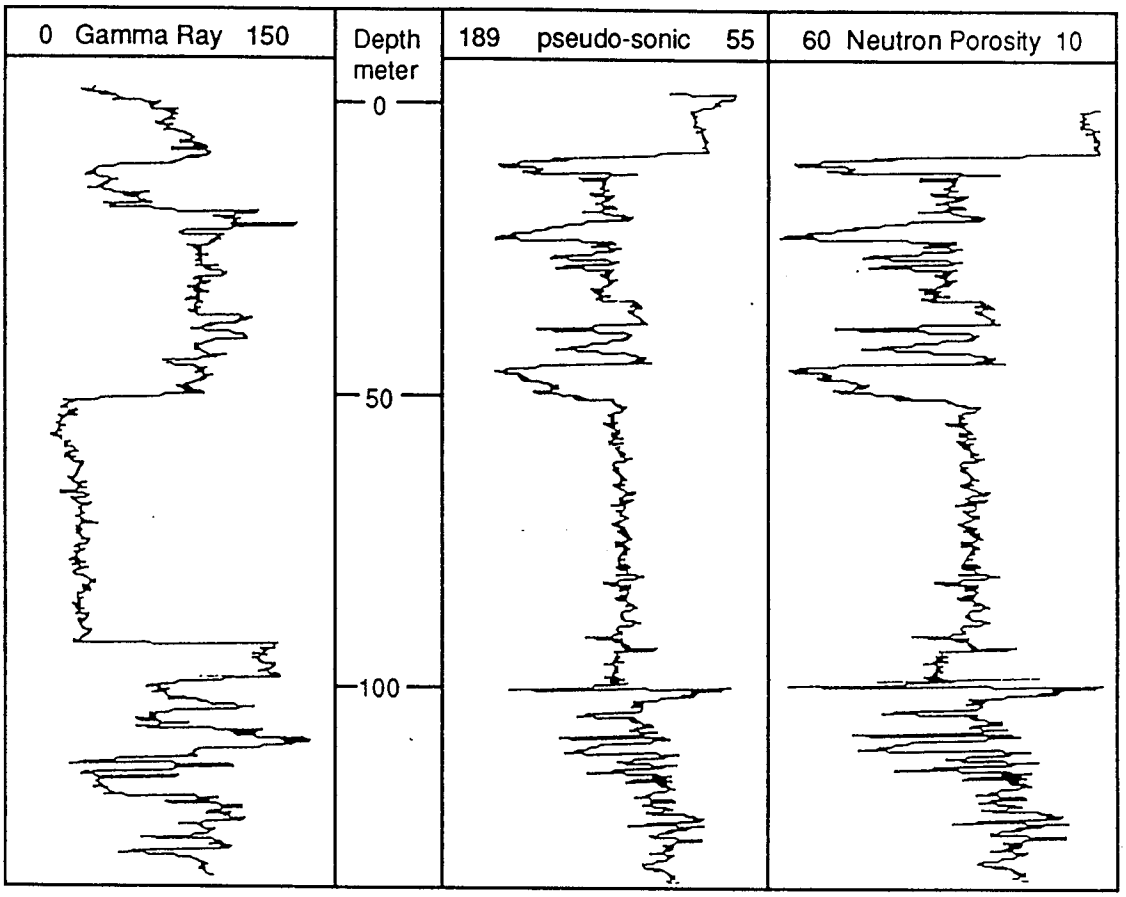

Figure 17. Comparsion of pseudo-sonic log and Neutron Porosity log, The pseudo sonic log predicts acoustic impedence contrasts at the top and bottom of the channel sand.

Formation was friable and porous. The normal increase in velocity expected in going from shale to sandstone was evidently enhanced by the high water content and porosity of the shales. Had there been much overburden, the shale would most likely have been compacted and dehydrolized, which would have decreased the acoustic impedance contrast between the channel sand and the adjacent shales.

The frequency of the first-order Ricker wavelet used in making the synthetic seismic trace varies depending on the dominant frequency of the reflecting events on the each of the seismic sections. A 95-Hz wavelet was used for line 1. Line 3 had much higher frequencies and a 200-Hz wavelet was used to make the synthetic seismogram. Line 4 had reflection information right at 100-Hz within the interval that was logged. A 100-Hz wavelet was used for the synthetic seismogram on line 4.

INTERPRETATIONS

Line 1

Walkaway 1 was shot on August 16, 1988, next to the site of the Haberer well (Figure 4). In this test the geophones were planted in the ditch next to the road and the shot holes were drilled on the road. The Graneros Shale was at the surface in the ditch. Open, 110-Hz, 220-Hz, and 340-Hz low-cut filters were tested (Figures 18 and 19). Source-receiver offsets were tested from 4 ft (1.2 m) to 388 ft (118 m). The data show reflection information exceeding 170-Hz above 0.150 sec (Figure 19). Reflections above 130-Hz were recorded from the Stone Corral Formation at a depth of approximately 215 m. The results of this first test indicate that the channel sand could be visible with reflection seismology at this site.

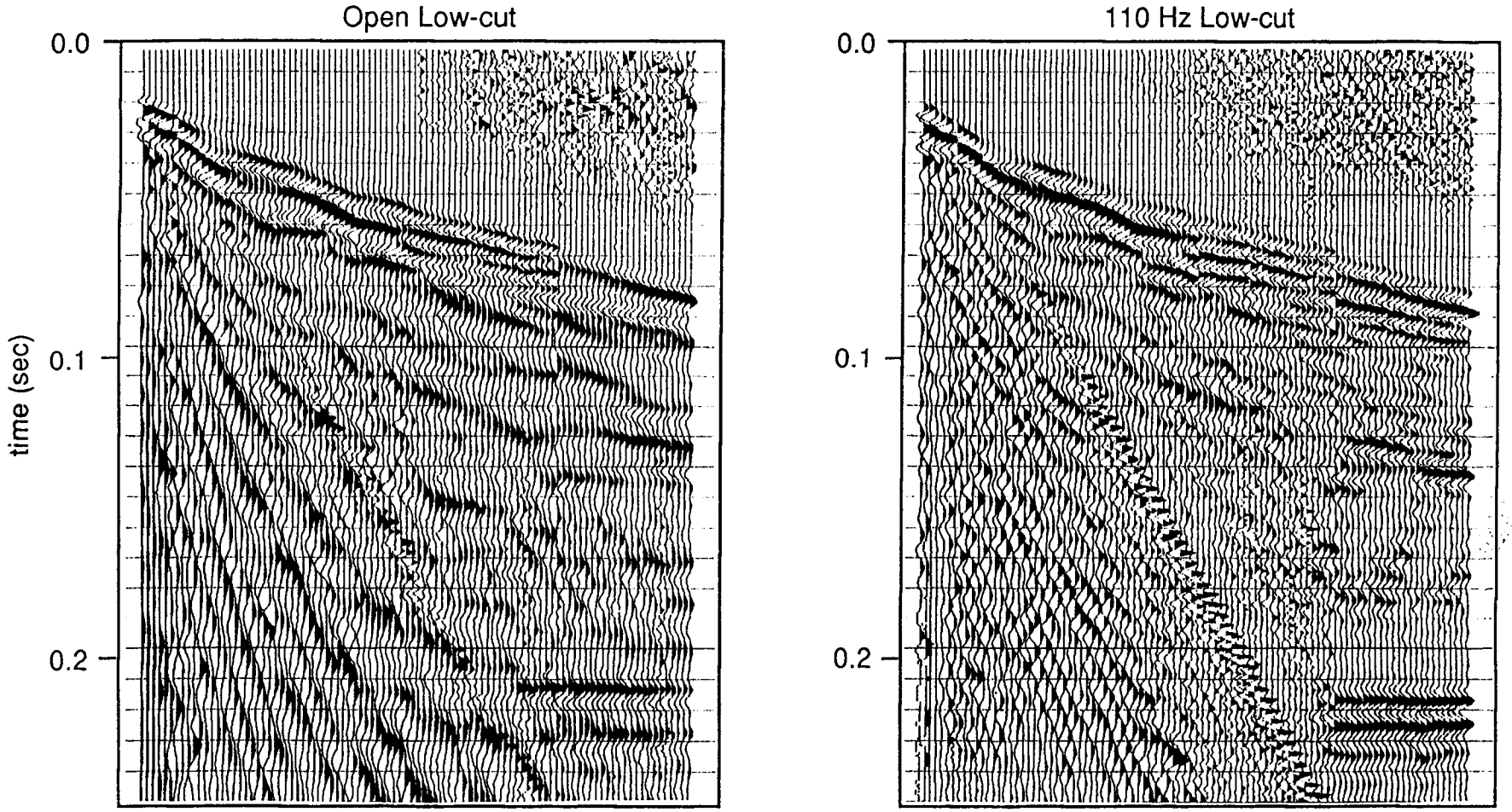

Figure 18. Walkaway tests next to the Haberer well.

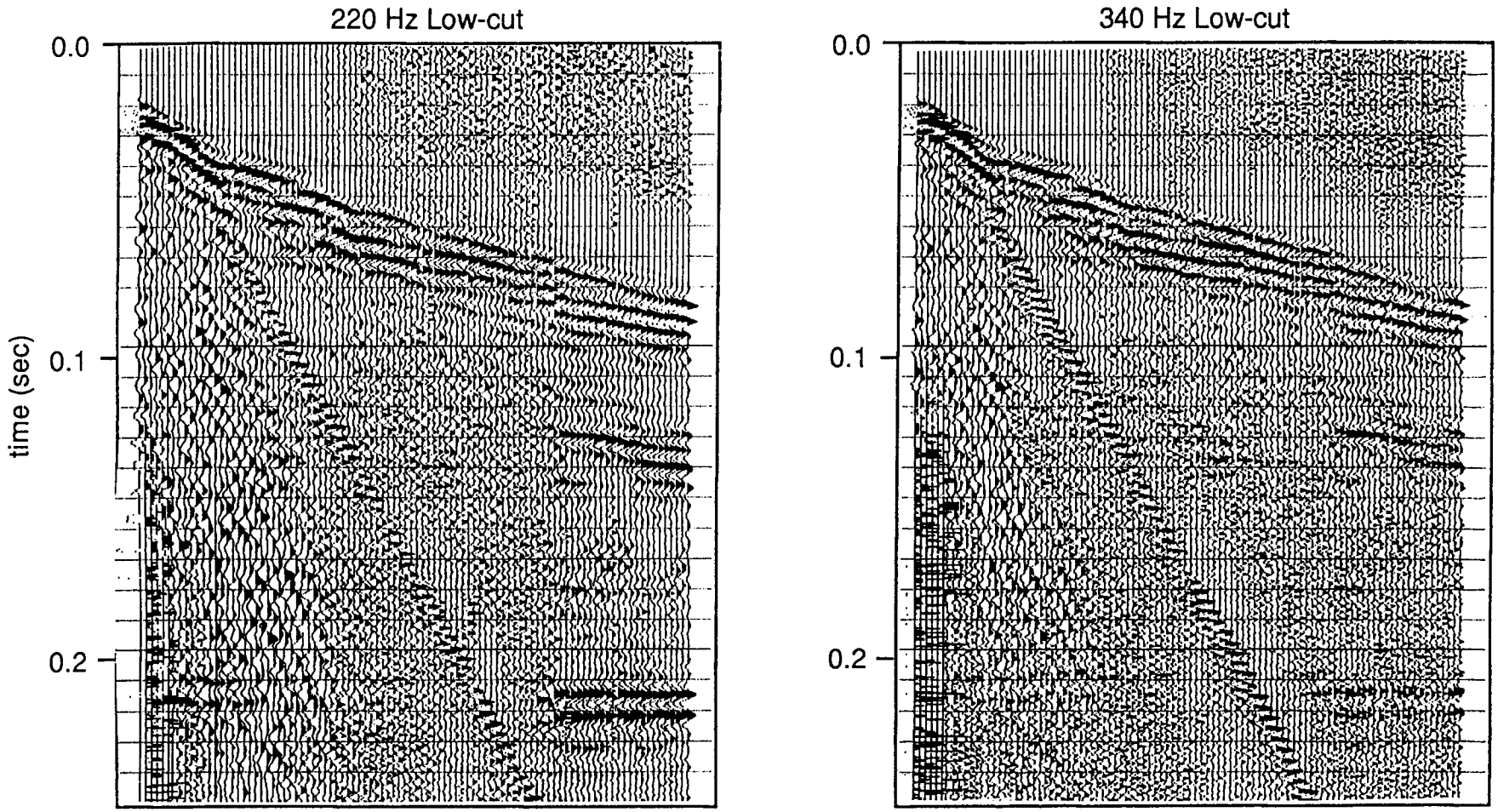

Figure 19. High frequency reflections are identifiable on the walkaway shot with 340 Hz low-cut filters.

Line 1 was shot 100 m south of walkaway 1 in the Saline River Valley on August 24, 1988. The surface is Pleistocene terrace deposits. The site was chosen because it was relatively flat and elevation measurements were not needed. The receiver spacing was 2.5 m and the offset from the source to the nearest receiver was 15 m. The offset from the source to the far receiver was 72.5 m. Two 100-Hz geophones were spaced inline 1.5 ft (0.5 m) apart to help cancel the air-coupled wave from the source. The offset window is shown in Figure 19. Starting at the south end of the line, shot holes were drilled in the ditch adjacent to the road. Shot holes drilled from the middle of the line to the north end of the line had to be drilled in the road because the truck could not drive any further in the ditch.

The frequency of the data was lower than anticipated. The reflection at 0.12 s is only 90-Hz (Figure 20). On the walkaway shot a week earlier, reflections with frequencies of 170-Hz were seen at times greater than 0.12 s. Also, the data quality was worse on the north end of the line. The drop in data quality coincided with a change in the position of the source from in the ditch to on the road.

The reflector at 0.12 s is interpreted as the base of the channel sand. The sands below the channel cannot be separated from the reflection at the base of the channel. The top of the channel is visible at 0.085 s. The synthetic seismogram created using information from the Haberer well shows that at a frequency of 90 Hz, the series of acoustic impedance contrasts associated with sands directly below the channel sand cannot be resolved (Figure 21). The synthetic seismogram matches the field data and supports the interpretation. The reflector at 0.21 sec is the Stone Corral Formation. The reflection at 0.16 sec is from impedance contrasts within the Nippewalla Group.

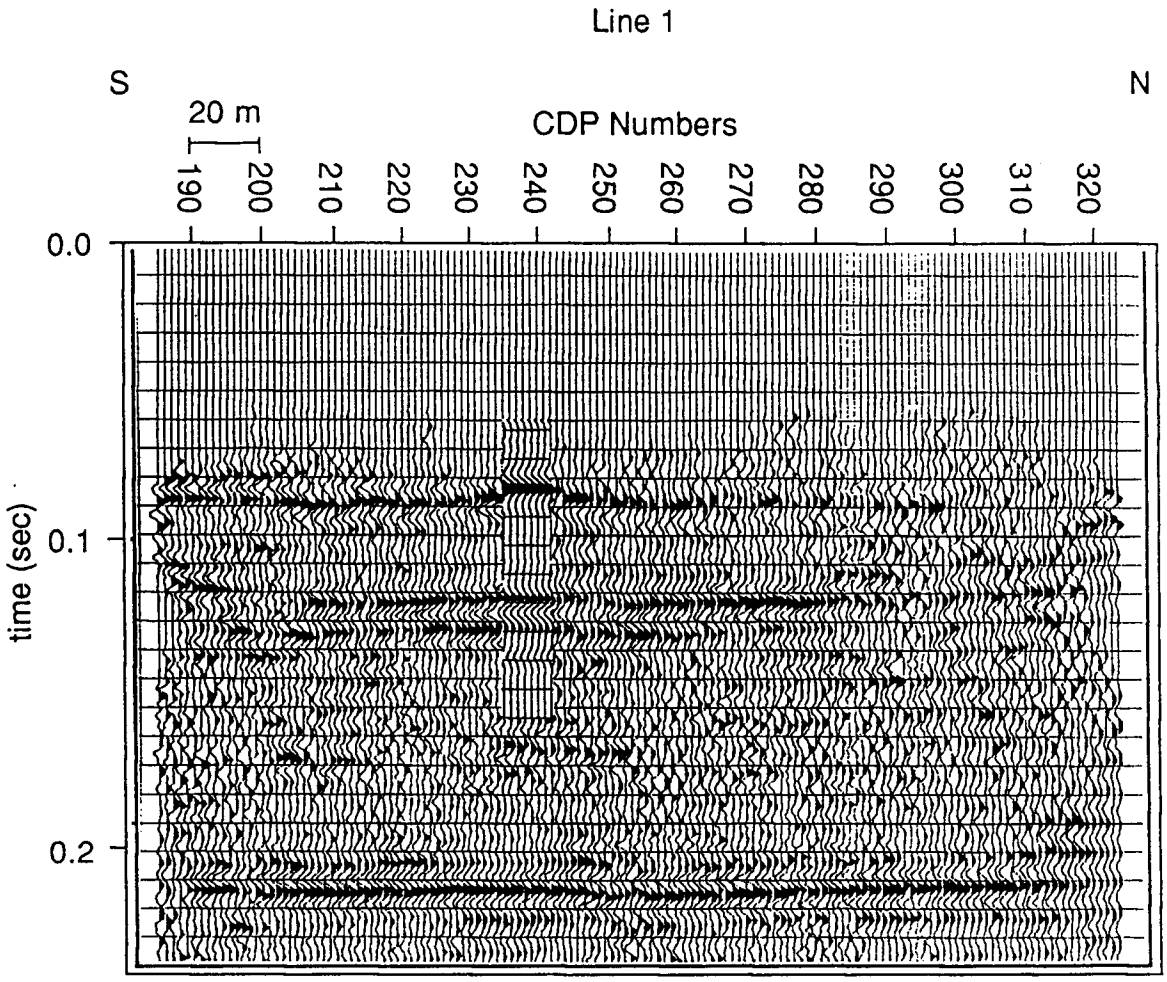

Figure 20. Reflections on line 1 have dominant frequencies between 90 and 100 Hz.

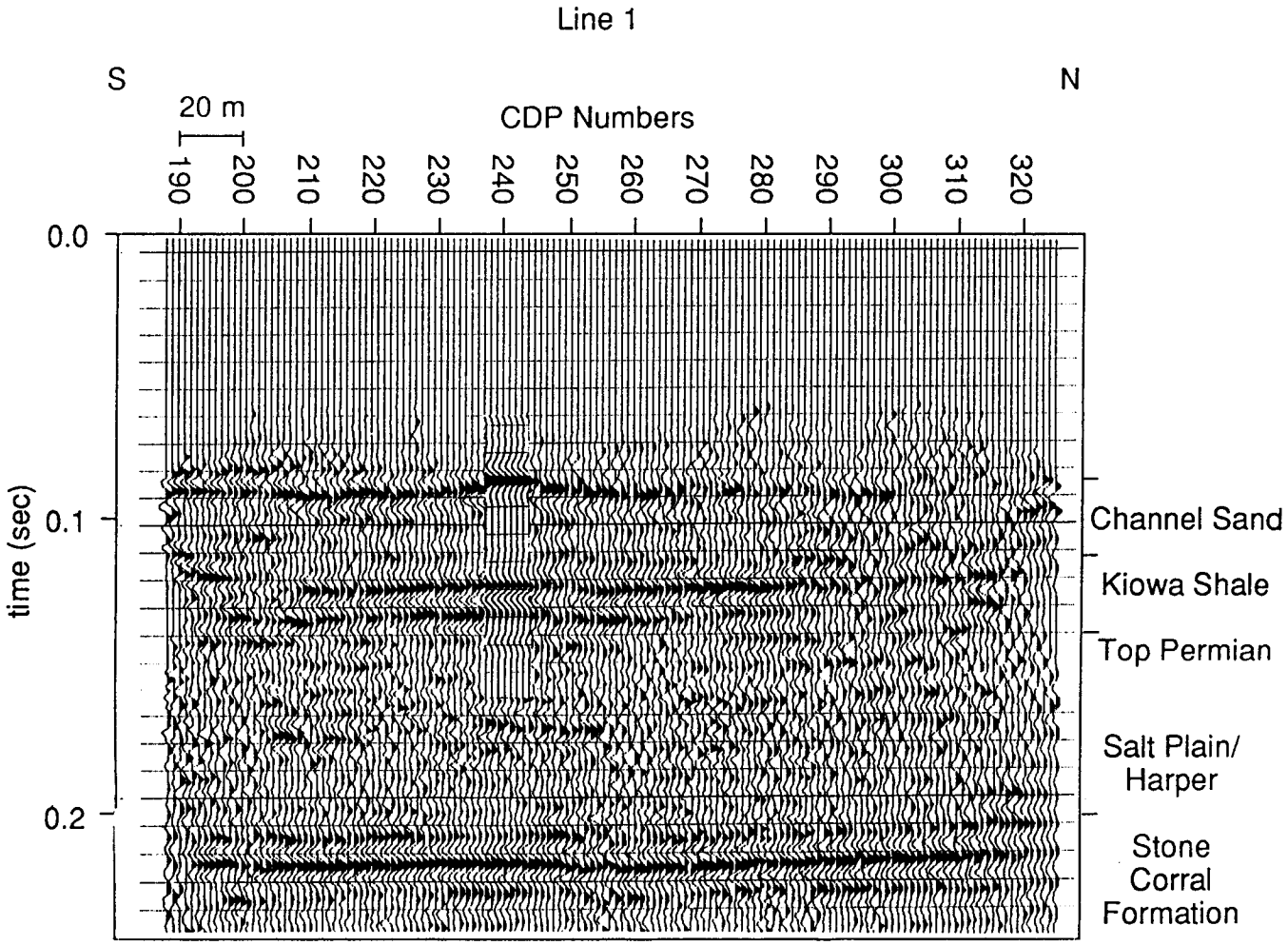

Figure 21. Interpretation of line 1. The synthetic seismogram supports the interpretation.

Drought conditions had existed all summer in the study area and the alluvium was very dry. The near-surface conditions, dry unconsolidated alluvium, on which the line 1 was shot was the variable that changed from the shooting of the walkaways a week earlier. The drop in the dominant frequency is most likely associated with the attenuation of energy in the dry, unconsolidated alluvium. Variation in the thickness of the alluvium caused static problems on the CDP gathers. The reflection from the Stone Corral Formation was used to monitor static corrections applied to the data during processing. Better data quality would be expected if the drought conditions had not existed and the water table had been close to the surface in the alluvial valley. Lower attenuation of high frequency energy and better source coupling have been noted in areas where the near surface is saturated (Hunter et al., 1984; Rick Miller, personal communication 1989).

The thickness of the channel sand was reduced in 5 ft (1.52 m) intervals in the pseudo-sonic log and synthetic seismic traces were made at each interval. The series of synthetic traces were plotted together to model a hypothetical pinchout of the channel sandstone. The model shows the pinchout as a thinning of the transparent zone between the reflection at the top of the channel and the reflection from the Kiowa Shale (Figure 22).

Line 2

Walkaway 2 was shot on March 17, 1989, in an east-west direction along the county road down the middle of sec. 26, T. 12 S., R. 15 W. The site, 2 mi (3.2 km) south of the Haberer well, was picked because the isopach map of the channel sand predicts that the sandstone thins by 15 to 25 m (Figure 4). The site is also higher in the stratigraphic section than the site for line 1. The Greenhorn Limestone is at the surface. Bad weather

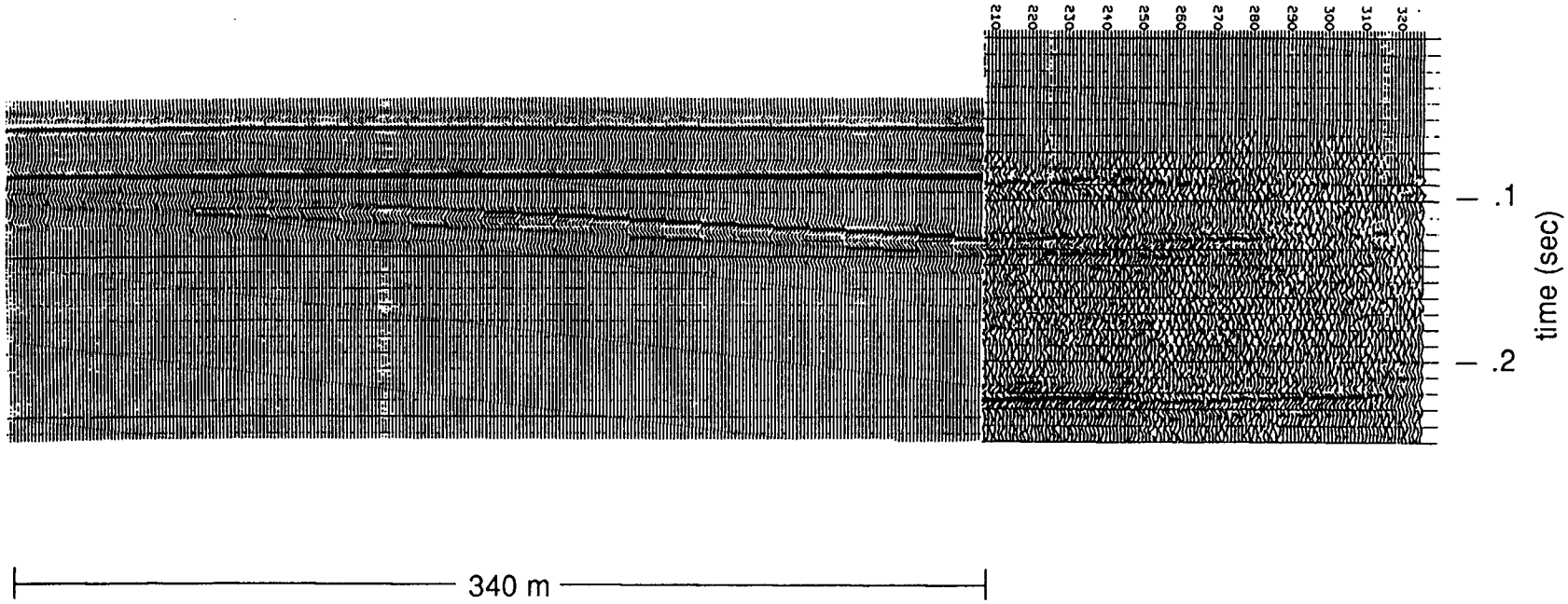

Figure 22. A pinchout of the channel sand could be recognized as a thinning of the transparent zone.

conditions contributed to the low signal-to-noise ratios seen in the data. The weather changed from warm and sunny on the day before to cold, wet, and windy on the morning of the 17th. The temperature was 35°F, freezing rain was pelting the seismic crew, and the wind was gusting at 30 mph. Source-receiver offsets were tested from 3 m to 108 m. The field plots of the walkaway tests did not show any reflection information. Refractions, ground roll, air-coupled wave, and "ringing refractions" are the only coherent events that can be recognized on the walkaways (Figure 23). The high level of noise is especially apparent on the far offsets. Parameters were chosen despite the lack of reflection information, and the line was shot hoping that processing could bring out reflections not seen on the field plots.

Stacked refractions on the final section of line 2 show the effect of the change in topography (Figure 24). As the elevation decreases, the travel time from the surface to the refractor decreases and the stacked refraction events appear higher on the section. This influence is also seen on the Stone Corral reflection at 0.24 sec on the east end of the line. At the west end of the line, the Stone Corral reflection barely appears on the record, but as the elevation decreases by 8 m, the reflection becomes more apparent on the east end of the line. There are several poor coherent events between CDP 270 and CDP 310 from 0.1 sec to 0.2 sec. that may have been more readily interpreted had the amount of random noise been less.

The stacked section of line 2 indicates that the walkaway tests were reliable. Processing did not bring out any significant reflection information. Coherent linear noise seen on the walkaways previously seem to be masking reflection information expected at the same arrival times. F-k filtering was used to remove linear noise with velocities of 1250 m/s and

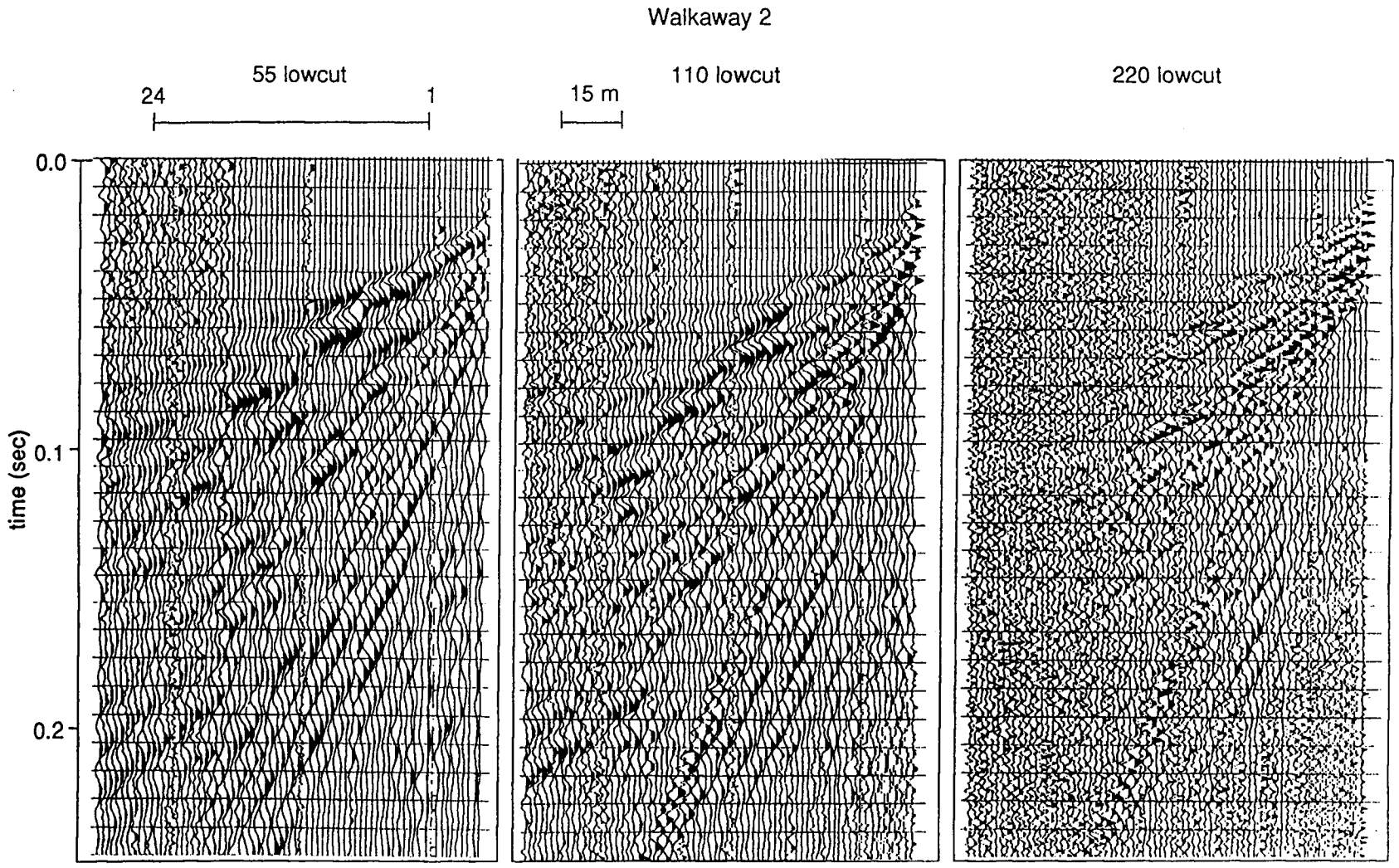

Figure 23. Reflections are not apparent with all the linear coherent noise and environmental noise.

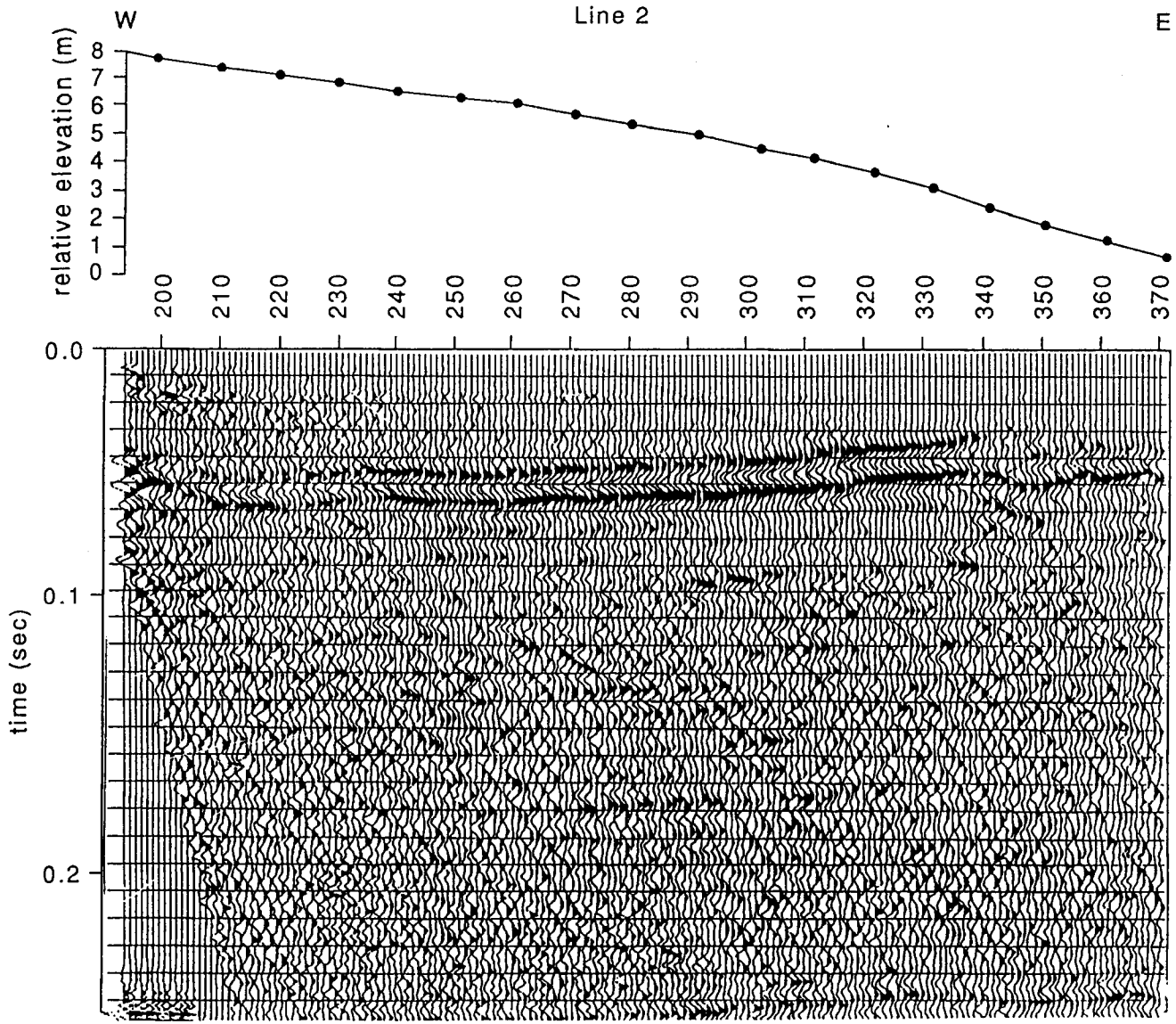

Figure 24. Reflections are not apparent on the CDP section of line 2.

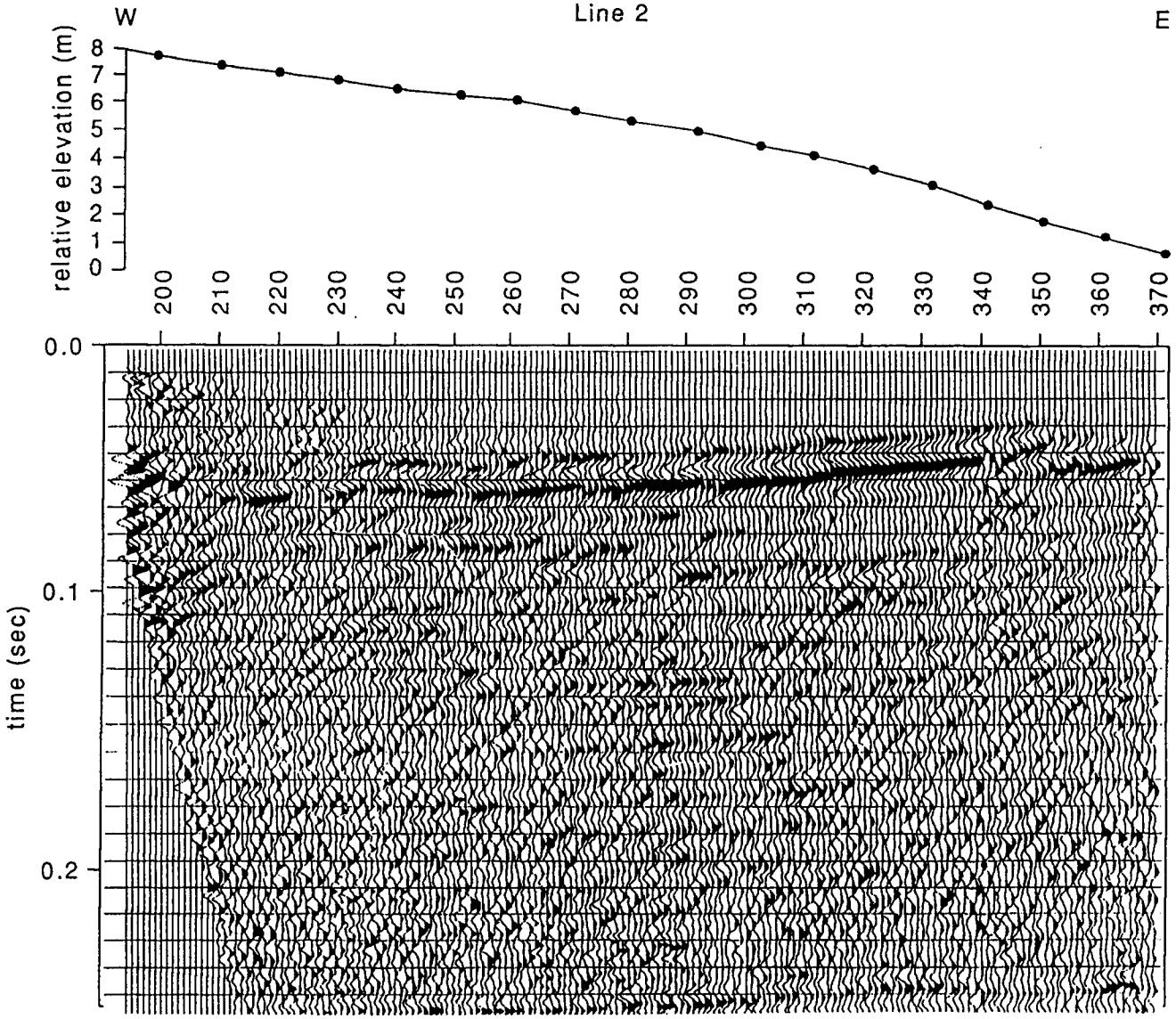

Figure 25. F-k filtering did not substanially improve the reflection information.

1530 m/s. After filtering, the same processing steps were applied to the f-k filtered field files. The final section of the f-k filtered data looks a little less noisy than the previous section (Figure 25). The f-k section does not reveal any reflections not seen on the band pass filtered section. A comparison of field files before and after F-K filtering showed that the filter had removed linear noise at the filtered velocities (Figure 11). The lack of coherent reflection events from file to file after F-K filtering indicates that A/D conversion had been saturated with coherent and random noise. Reflection information was not recorded above this high level of noise. The 12-bit A/D converter did not have enough dynamic range to record the signal under such noisy conditions.

Line 3

After shooting line 2 the weather conditions improved and by late afternoon it was warm and sunny again. Because low-frequency data and bad data had been obtained from sites in the alluvial valley of the Saline River and on top of the Greenhorn Limestone, respectively, the site of walkaway 1 was revisited. The Graneros Shale is at the surface at this site. A new walkaway test was set up with both geophones and shot holes located in the ditch on the west side of the road. The results showed that 200-Hz reflection information could be recorded within the window of interest (Figure 26). The parameters for line 3 were then chosen. The receiver and shot spacing were set at 2 m. Three 40-Hz geophones were planted in line in a 2 ft (.6 m) array to help cancel out the air wave from the source. The minimum and maximum source-to-receiver offsets were 12 m and 58 m., respectively. The optimum window selected is shown on Figure

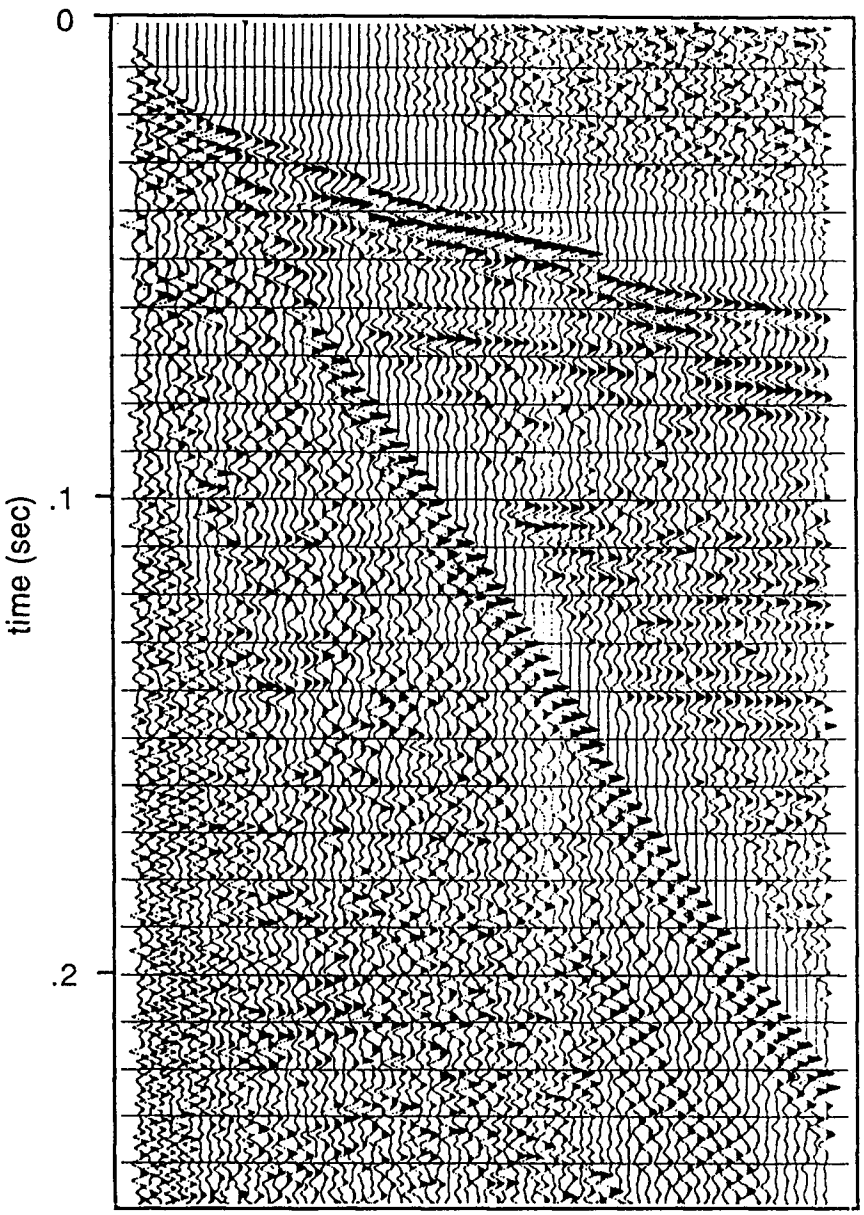

Figure 26. Reflections from both the top and bottom of the channel sand are apparent on the walkaway.

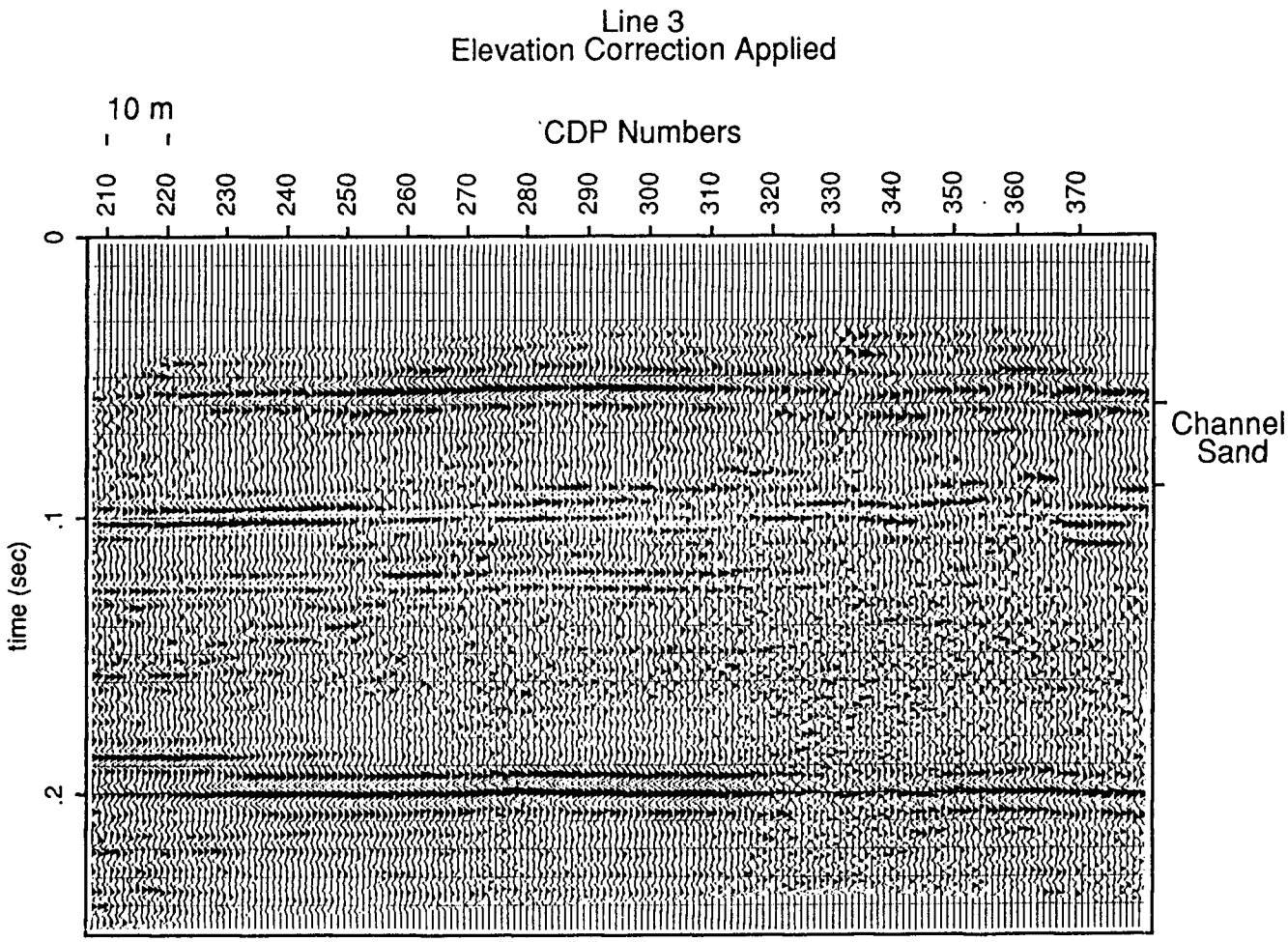

Figure 27. The channel sand is readily apparent at the top of the CDP section.

24. Two-hundred twenty Hertz low-cut and 1000-Hz high-cut filters were used.

The top of the channel sand can be seen at approximately 0.6 sec. on Line 3 (Figure 27). The base of the channel is seen at 0.9 sec. The reflection at the base of the channel is 200 Hz on the south end of the line. Several reflections can be seen below the Dakota Formation on the south end of the line. As you move north on the line, the frequency and data quality drop. At CDP 233 the frequency drops on the reflection at the base of the channel sand. At CDP 255 data quality drops on the reflection at the base of the channel sand. The changes coincide with a gradual change in topography and surface conditions (Figure 28). The severe drop in data quality between CDP 320 and CDP 350 is due to an increase in the thickness of alluvium and bad surface plants. A cement pad and two shallow shot holes lowered the number of shots taken through this area lowering the fold as well. Geophones were planted in fresh exposures of the Graneros Shale on the south end of the line. Pleistocene alluvium deposited unconformably on the Graneros Shale gradually increases in thickness to the north. Just over the crest seen on the topographic profile the Graneros is again at the surface, coinciding with an increase in data quality at the north end of the line.

The reflections from other sandstones observed below the channel sand on well logs from the Haberer well are visible. The reflections between 0.1 s and 0.12 s are from the Kiowa Shale. The reflection at 0.12 s is interpreted as the contact between the Kiowa Shale and the Cedar Hills Sandstone. The reflection at 0.19 s. is the Stone Corral Formation. A synthetic seismogram made using a 200-Hz wavelet shows that the base of the channel sand and sandstones within the Kiowa Formation can be

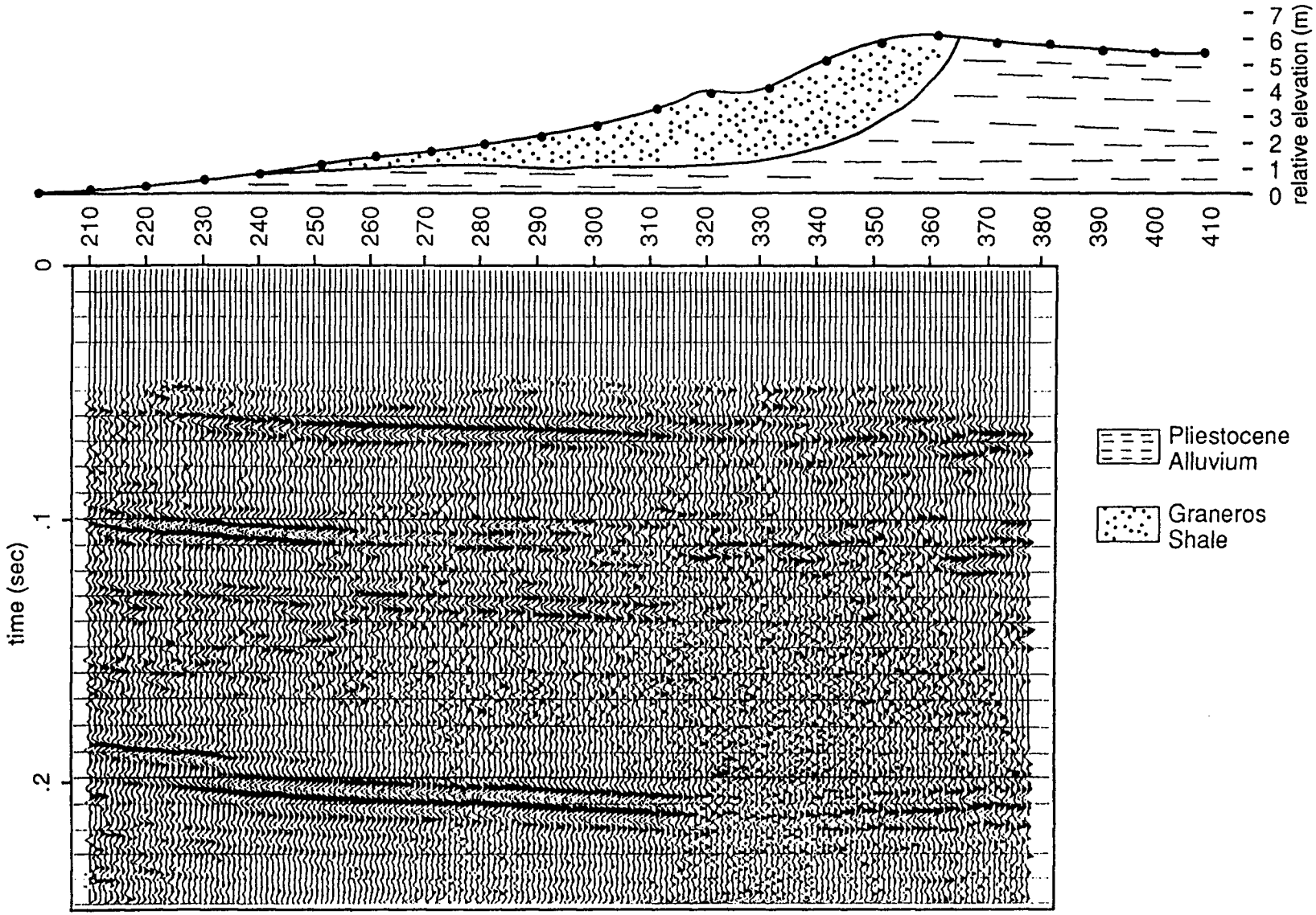

Figure 28. Changes in reflection quality can be associated with changes in near surface geology.

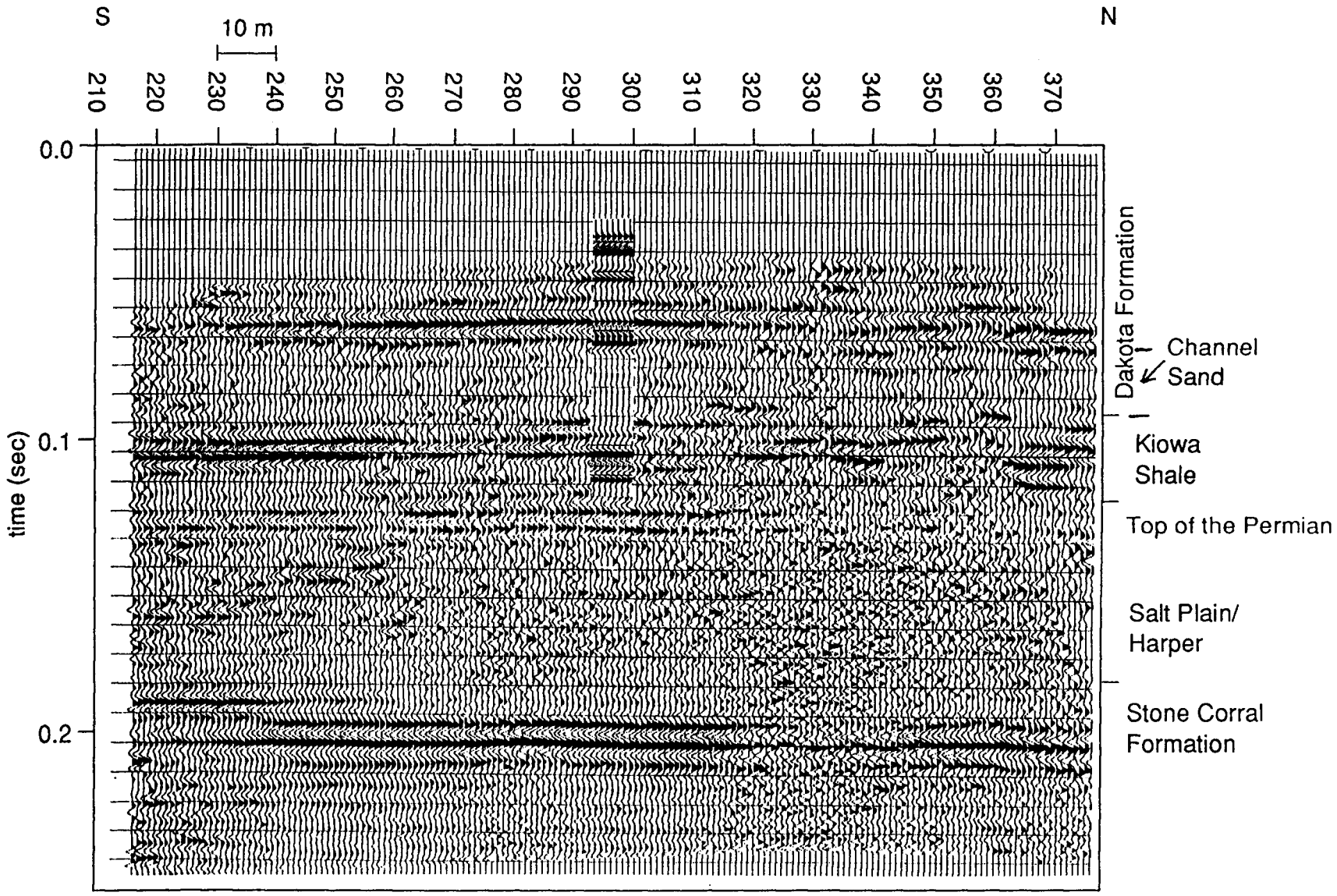

Figure 29. Interpretation of line 3. The synthetic seismogram supports the interpretation.

resolved. The synthetic seismogram matches the field data and supports the above interpretation (Figure 29).

The high frequency data of line 3 not only allows easy interpretation of the channel sand in question, but also the contacts between the Dakota Formation, Kiowa shales and sandstones, and the underling Permian beds can be resolved. A continuation of line 3 to the north would most likely be capable of resolving the pinchout of the channel sand and changes in the relationships between Lower Cretaceous rocks and the underlying Permian rocks.

Line 4

Line 4, at the Brungardt site, was shot on July 25, 1989. Stations were flagged in an east-west direction 10 m south of the Brungardt well. Three 40-Hz geophones were planted at each station. Spacing on the walkaway was 2 m. The walkaway tested source-receiver offsets from 2 m to 208 m. Times after the arrival of the air blast were saturated with low-frequency ground roll on the walkaway shot with open low-cut filters (Figure 30). Low-cut filters were set at 110 Hz, and high-cut filters were set at 250 Hz. Noise from a front-end loader working at the east end of the line can be seen on the walkaway (Figure 31). Acquisition of data must stop and wait for such disturbances to end. Reflections are visible on the far offsets. The sampling rate was changed to 0.5 ms so that reflections from the Stone Corral Formation could be recorded. The system is limited to 1000 samples per trace which would give 0.25 s of data at 0.25 ms sampling and 0.50 s of data at 0.50 ms sampling. At this site the Stone Corral reflection was at 0.33 s.

The near source-to-receiver offset was set at 92 m and the far source-to-receiver offset was set at 184 m. These offsets are shown on Figure 30.

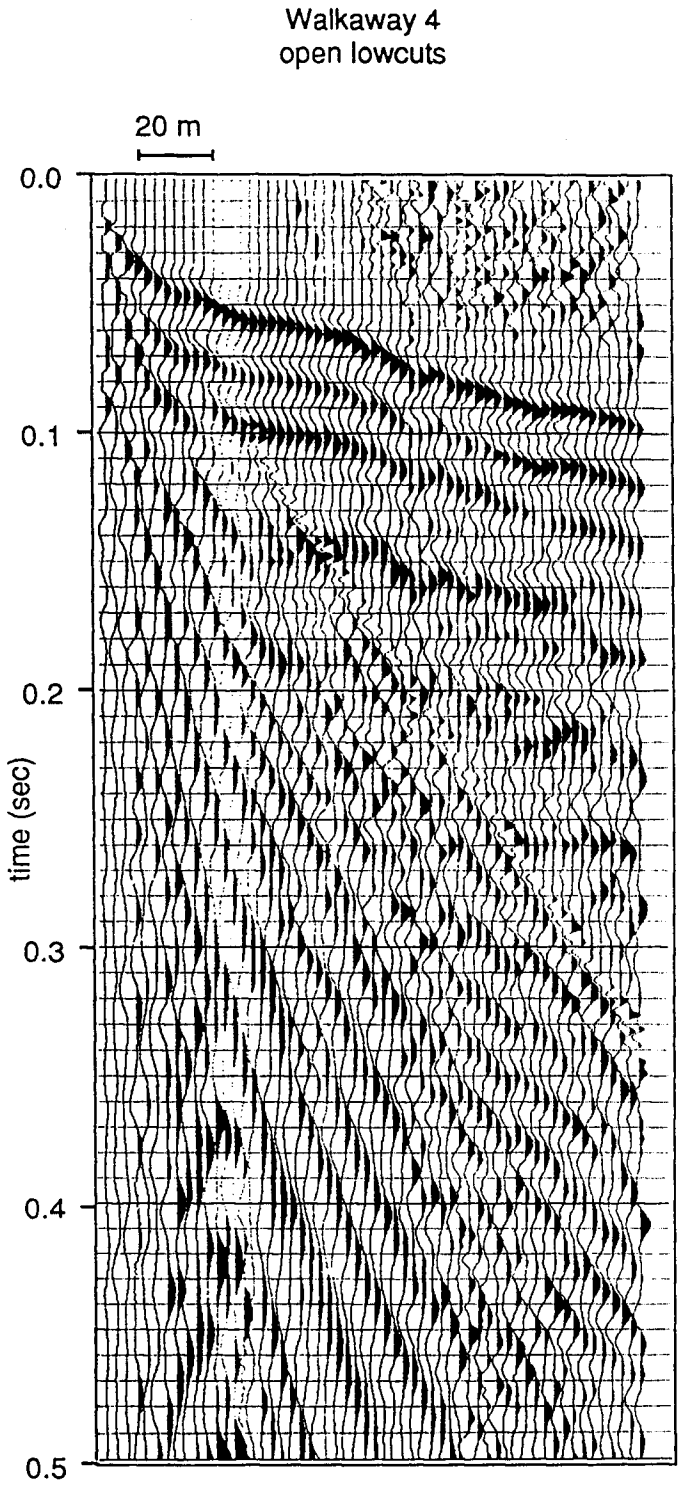

Figure 30. Low frequency ground roll at the Brungardt site.

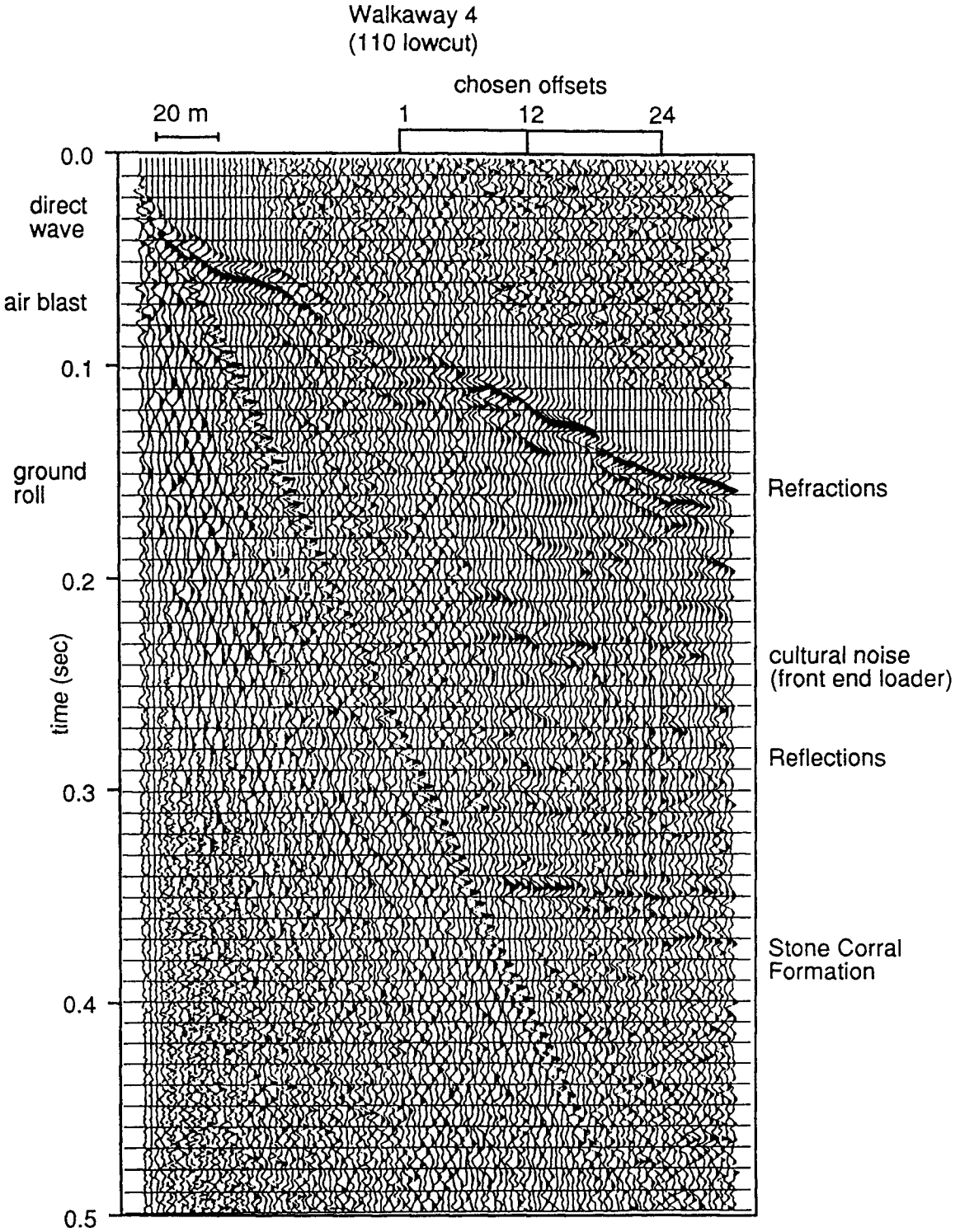

Figure 31. Walkaway test from the Brumgardt site. Large offsets were used to get reflection information

Receiver and shot locations were placed every 4 m. The low-cut and high-cut filters were set at 110 Hz and 220 Hz, respectively. Sampling rate remained at 0.5 ms. Total record length was 0.5 s.

Eighty-two stations were flagged. Shot holes were drilled from station 107 to station 135. Receivers were located from station 130 to station 181. Receivers were planted on the edge of the road from station 130 to station 152. Receivers located at stations 153 and higher were planted in the road ditch on the side of the road (Figure 32). All the shot holes were drilled in the road.

Because of the large source-receiver offsets, the first reflections are seen at 0.10 s (Figure 33). A zone of several broken up reflectors runs from 0.10 s to 0.20 s. A more coherent reflector can be seen at 0.21 s. The most coherent reflectors are at 0.26 s and 0.33 s. Reflections from Cretaceous formations (0.10 to 0.25 s) are not as coherent as deeper reflections from the Nippewalla Group and from the Stone Corral Formation.

The reflection from the Stone Corral Formation increases in data quality and frequency from CDP 243 to CDP 273. The changes coincide with changes in the surface where the geophones are planted. The more CDP receivers planted in the road ditch rather than on the road, the better the reflection (Figure 32).

At this location the channel sand is not present. The base of the Dakota Formation is at a depth of 188 m. A sand only 4.5 m thick is at the base. There are several sands within the Dakota Formation ranging from 1 m to 16 m in thickness (Figure 3).

The reflections on line 4 have a dominant frequency of 100 Hz. The thin sand lenses at the base of the Dakota Formation can not be resolved with 100 Hz wavelets. The contact between the base of the Dakota

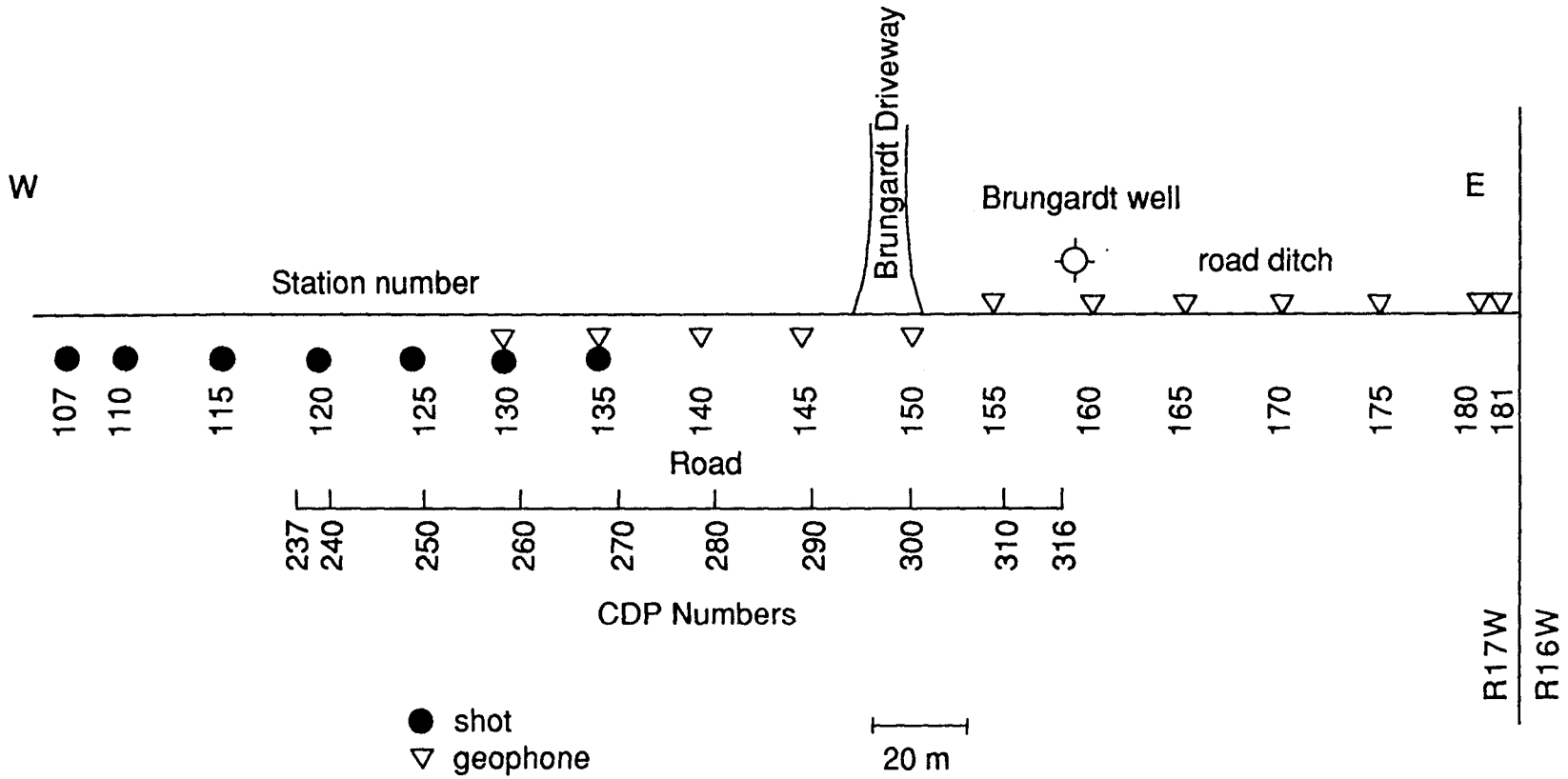

Figure 32. Geophones planted in the road ditch are associated with higher frequency and better quality reflections on the CDPstacked section.

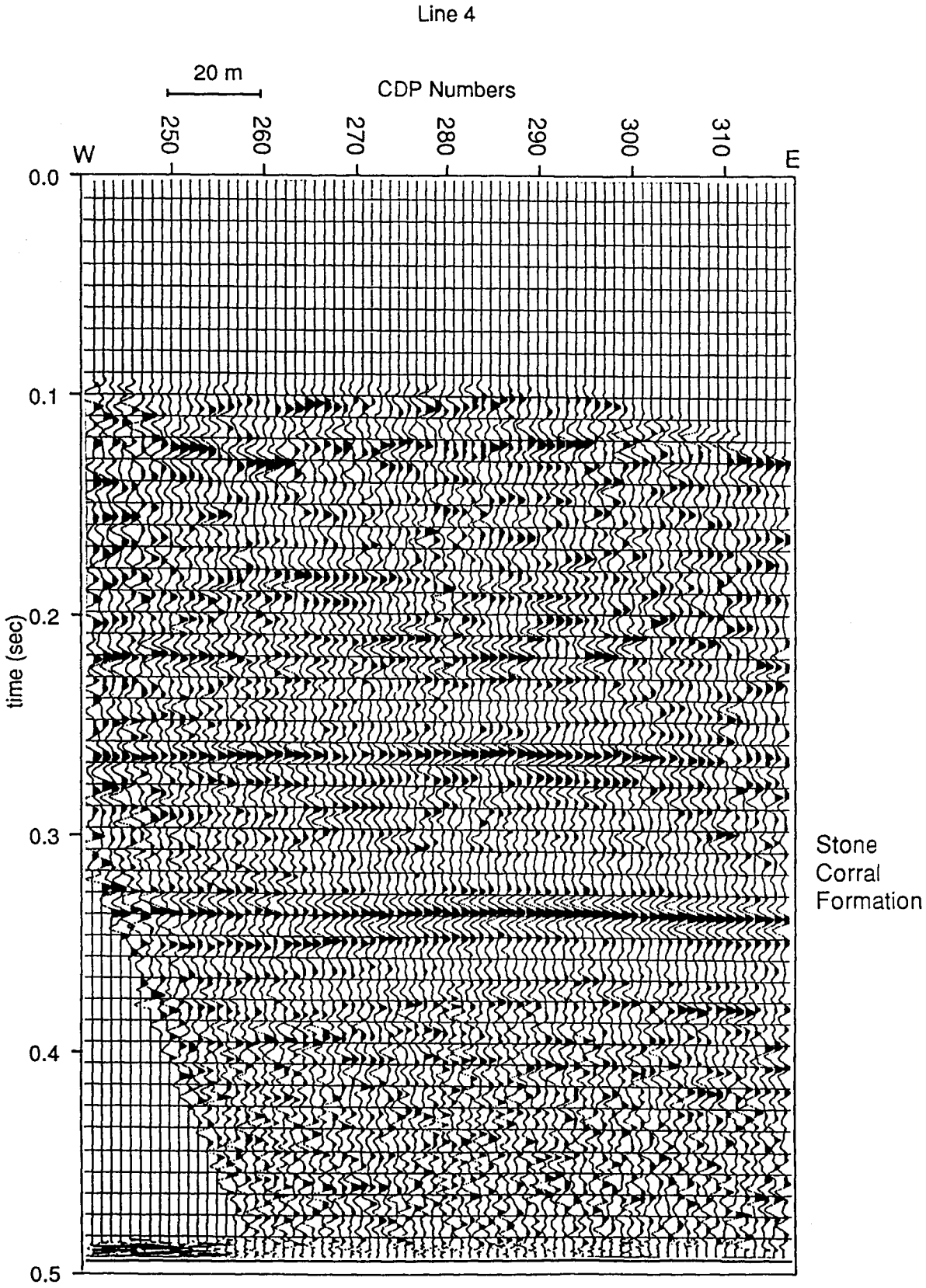

Figure 33. Frequency of the reflection at .33 s increases to the east.

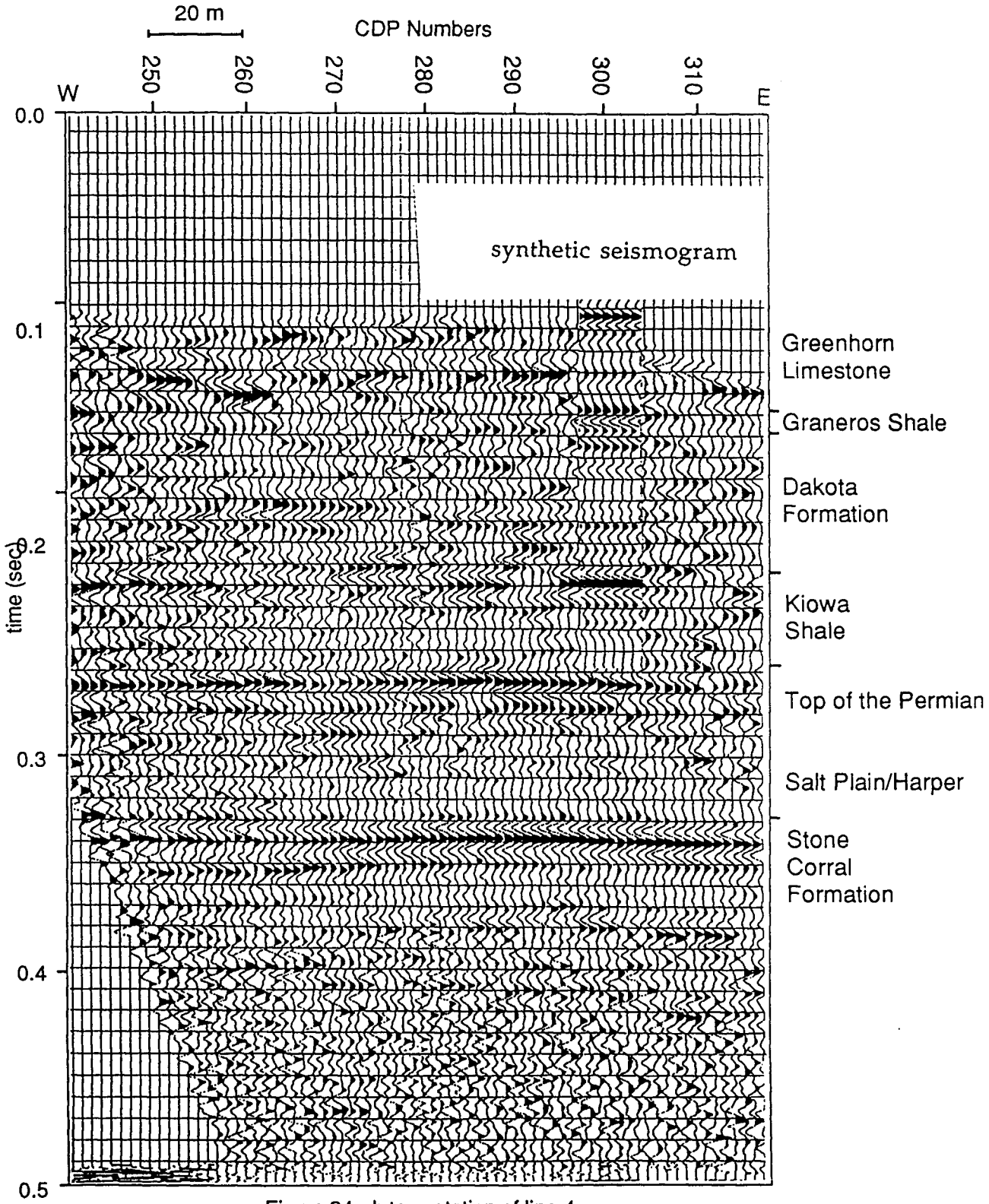

Figure 34. Interpretation of line 4.

Formation and the underlying Kiowa Shale has a sharp change in velocity shown on the sonic log from the Brungardt well and has definite kick on the synthetic seismogram made from the sonic (Figure 13). The synthetic seismogram was converted to SPEX format and spliced into line 4 (Figure 34). With the aid of the synthetic seismogram the base of the Dakota Formation can be identified at 0.21 s. Reflections from the Greenhorn Limestone, Graneros Shale, and Dakota Formation are all identified using the synthetic seismogram. The reflection at 0.26 s is interpreted as the top of the Permian. The Stone Corral Formation is easily recognized at 0.33 s. Modeling show that if a 30-m sandstone had been present at the base of the Dakota Formation it would have been resolvable with the frequencies obtained on line 4 (Figure 35).

CONCLUSIONS

1. High-frequency reflections interpreted as the top and bottom of the channel sandstone at the base of the Dakota Formation can be confidently identified on CDP stacked seismic sections.

2. Sandstones below the base of the Dakota Formation, including the Longford Member of the Kiowa Shale and the Cedar Hills, were resolvable and identified where reflections with frequencies above 180 Hz were recorded.

3. Resolution and data quality were site dependent. Best results are obtained when the data is collected on fresh exposures of Graneros Shale. Reflections of 200 Hz and higher were recorded at these sites. Sites that have dry alluvium at the surface are less desirable. These sites yielded reflection frequencies lower than 100 Hz. The worst sites are those directly

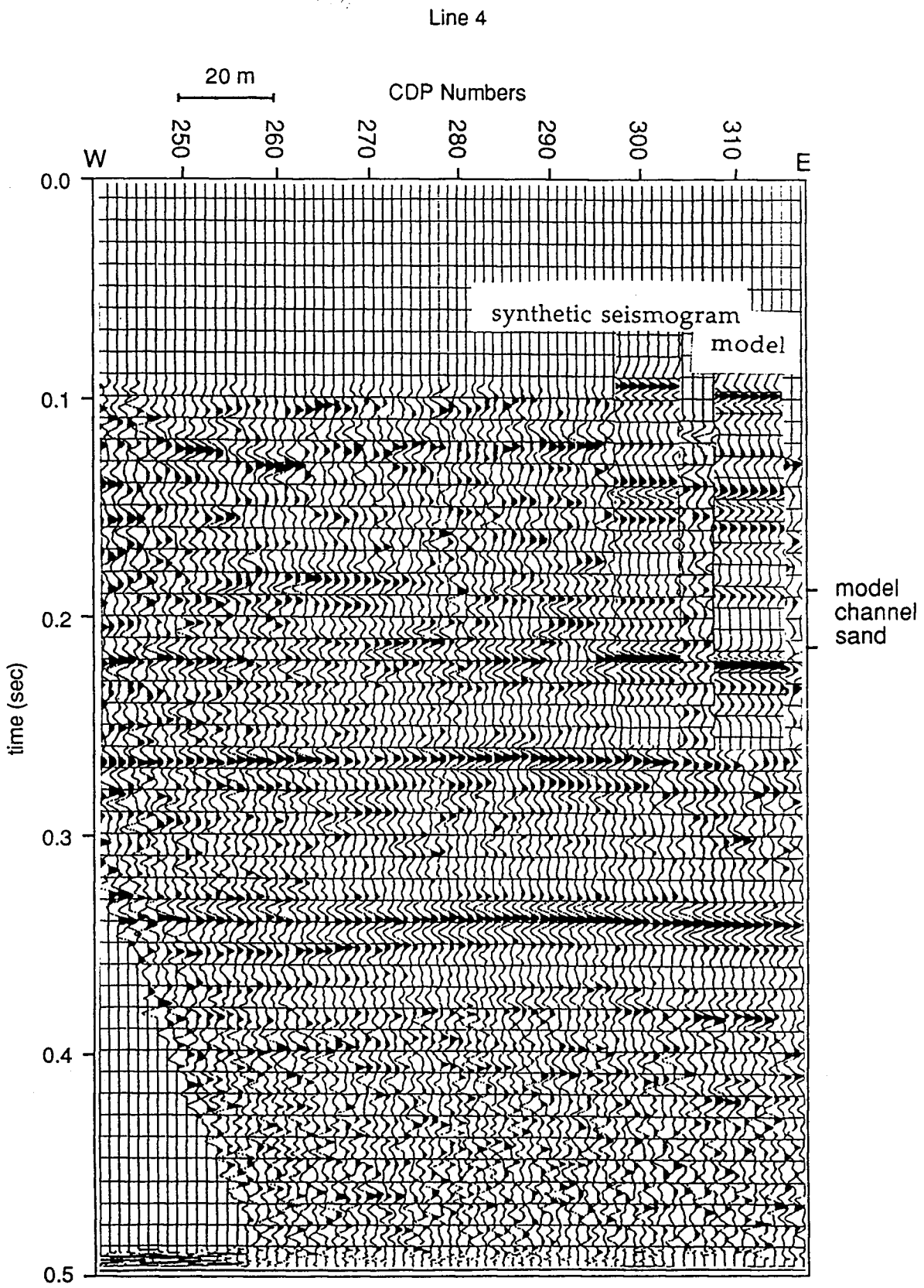

Figure 35. Channel sand would be approved as a transperant zone if present at this location.

on the Greenhorn Limestone. Low frequencies were recorded where the ground surface was stratigraphically higher than the Greenhorn Limestone.

4. The intermediate results obtained on lines 1 and 4 can be expected at most sites in central and western Kansas. At these intermediate sites the base of the Dakota Formation can be detected. If a channel sand similar to the one penetrated by the Haberer well is present it will have recognizable reflections from both the top and bottom interfaces. The level of resolution, however, will not allow the distinction of the base of the channel or base of the Dakota Formation from the underlying sandstones in the Kiowa Shale.

5. Geophones and shot holes located in the road ditch improved the resolution and the S/N ratio. Sources and receivers located on the road surface resulted in lower-quality data.

6. Record length and sampling rate adjusted to allow for the recording of reflections from the Stone Corral Formation allowed confident correlation of the four seismic lines. On a local scale it is acceptable to use the Stone Corral Formation for static corrections, which otherwise would be difficult. The seismic lines collected for this study can be used to help interpret seismic lines collected in the future. The characteristic reflection from the Stone Corral can easily be identified and used as a starting point to correlate seismic data.

7. The synthetic seismogram calculated from the Brundgardt sonic log greatly aided in the interpretation of line 4. The neutron porosity log, gamma ray log, and density log were used to create a pseudo sonic log for the Haberer well . The synthetic seismogram generated from the pseudo-sonic log aided in the interpretation of line 1 and line3. The neutron porosity log alone proved acceptable to calculate a pseudo-sonic log. Using the coefficients derived from the Brundgardt well logs, pseudo-sonic logs and

synthetic seismograms can be generated from available well information in areas where seismic data are to be collected.

8. The F-K filtering program used on line 2 removed linear noise without creating artifacts. Linear moveout at the velocity of the noise to be removed before 2-D Fourier transformation and very smooth tapering were instrumental in not creating artificial coherency. The success of the filter indicates that if weather conditions had been better and some signal had been recorded with the linear noise, the filter could remove the noise increasing S/N ratio and allowing interpretation of the data. However, no amount of processing can uncover signal that was never recorded.

The low amount of signal recorded on line 2 was also a function of the dynamic range of the seismograph. The 12 bit fixed-point system has a potential dynamic range of 72 dB. This was not enough to record both the high amplitude coherent noise and any low amplitude signal that was present. F-k filtering could increase the number of sites where seismic reflection could detect the sandstone lenses in the Dakota Formation if the data were recorded with a seismograph with enough dynamic range to record both high amplitude coherent linear noise and low amplitude signal.

9. Areas stratigraphically higher than the Blue Hill Shale Member of the Carlile Shale have not been studied. As the depth to the Dakota Formation increases to the west, less energy and lower frequencies would be expected from reflections in the target interval. Thus the data would not be better than the intermediate quality seen on line 1 and line 4. Most likely the data quality and resolution would be lower.

REFERENCES

Bayne, C.K., Franks, P.C., and Ives, W., 1971, Geology and ground-water resources of Ellsworth County central Kansas: Kansas Geological Survey Bulletin 201.

Beebe, B.W., 1959, A case history of the Koelsh southeast pool, Stafford County, Kansas, a study in microseismics, in Hambleton, W.W., ed., Symposium on Geophysics in Kansas, Kansas Geological Survey Bulletin 137.

Care, J.L., Brooks, L., and Wallace, C.H., 1959, Geophysical case history of t he Engel pool, in Hambleton, W.W., ed., Symposium on Geophysics i n Kansas, Kansas Geological Survey Bulletin 137.

Dobrin, M.B., 1976, Introduction to geophysical prospecting: McGraw-Hill Book Co., New York.

Doveton, J.H., and Cable, H.W., 1983, Terralog. Terrasciences Inc., San Ramon, California.

Franks, P.C., 1975, The transgressive-regressive sequence of the Cretaceous Cheyenne, Kiowa, and Dakota Formations of Kansas, in Caldwell, W.G.E., ed., The Cretaceous System in the Western Interior of North America, Geological Association of Canada, Special Paper 13, p.469-521.

Hattin, D.E., 1965, Stratigraphy of the Graneros Shale (Upper Cretaceous) i n central Kansas: Kansas Geological Survey Bulletin 178.

Hunter, J.A., Pullan, S.E., Burns, R.A., Gange, R.M., and Good, R.L., 1984, Shallow seismic reflection mapping of the overburden-bedrock interface with the engineering seismograph- Some simple techniques, Geophysics, 49, p. 1381-1385.

KGS, 1986, Technical guidance document and program proposal to assess the water resources potential of the Dakota Aquifer in Kansas, along term multi-agency research program.

Knapp, R. W., and Steeples, D.W., 1986, High-resolution common-depth-point reflection profiling: Field acquisition parameter design, Geophysics, v. 51, p. 283-294.

Lindsey, J.P., 1989, The Fresnel zone and its interpretive significance, Geophysics: The Leading Edge, v. 8, no.10, p. 33-39.

Macfarlane, P.A., Doveton, J.H., and Coble, G., 1989, Interpretation of lithologies and depositional environments of Cretaceous and Lower

Permian rocks by using a diverse suite of logs from a borehole in central Kansas, Geology, v.17, p. 303-306.

Merriam, D.F., 1955, Stone Corral structure as an indicator of Pennsylvanian structure in central and western Kansas: Kansas Geological Survey Bulletin Survey 114, pt. 4, p 129-152.

Merriam, D.F., 1963, The geologic history of Kansas: Kansas Geological Survey Bulletin 162.

Myers, P.B., Miller, R.D., and Steeples, D.W., 1987, Shallow seismic-reflection profile of the Meers Fault, Comanche County, Oklahoma: Geophysical Research Letters, v. 14, no. 7, p. 749-752.

Plummer, N.V., and Romary, J.F., 1942, Stratigraphy of the pre-Greenhorn Cretaceous beds of Kansas: Kansas Geological Survey Bulletin 41, pt. 9, p. 313-348.

Ready, T.G., 1985, A high resolution seismic study Miami County, Kansas, M.S. Thesis, University of Kansas, 97 p.

Rupnik, J.J., 1959, A case history of the Dunes pool, Pawnee County, Kansas, in Hambleton, W.W., ed., Symposium on Geophysics in Kansas, Kansas Geological Survey Bulletin 137.

Seeber, M.D., 1985, An evaluation of the fifty-caliber machine gun as a high-resolution seismic source for the exploration of shoestring sandstones, M.S. Thesis, University of Kansas, 75 p.

Sheriff, R.L., 1977, Limitations on resolution of seismic reflections and geologic detail derivable from them, in C.E. Payton, ed., Seismic stratigraphy-applications to hydrocarbon exploration: AAPG Memoir 26, p. 3-14.

Sheriff, R.L., 1984, Encyclopedic Dictionary of Exploration Geophysics. Society of Exploration Geophysicists, Tulsa, OK.

Sheriff, R.L., 1985, Aspects of seismic resolution, in O.R. Berg and D.G. Woolverton, ed., Seismic stratigraphy II an integrated approach: AAPG Memoir 39, p. 1-10.

Steeples, D.W., Miller, R.D., and Knapp, R.W., 1987, Downhole .50-caliber rifle--an advance in high-resolution seismic sources, [Exp. Abs.]; in Technical Program Abstracts and Biographies: Society of Exploration Geophysicists 57th Annual Meeting, p. 76-78.

Steeples, D.W. and Miller, R.D., 1988, Seismic reflection methods applied to engineering, environmental, and ground-water problems: proceeding

of the symposium on the application of geophysics to engineering and environmental problems.

Telford, W.M., Geldart, L.P., Sheriff, R.E., and Keys, D.A., 1976, Applied Geophysics. Cambridge University Press, Cambridge, Great Britain, 860 p.

Winchell, R.L., 1959, Law southeast pool-A successful seismic discovery in Graham County, Kansas, in Hambleton, W.W., ed., Symposium on Geophysics in Kansas, Kansas Geological Survey Bulletin 137.

Treadway, J.A., Steeples, D.W., and Miller, R.D., 1988, Shallow seismic study of a fault scarp near Borah Peak, Idaho: Journal of Geophysical Research, v. 93, no. B6, p. 6325-6337.

Widess, M.B., 1973, How thin is a thin bed, Geophysics, v.38, p.1176-1180.

Yilmaz, O., 1987, Seismic Data Processing; S.M. Doherty ed., in Series: I investigations in Geophysics, no 2, Edwin B. Neitzel, Series Ed.: Society of Exploration Geophysicists, Tulsa, OK.

Zeller, D.E., ed., 1968, The stratigraphic succession in Kansas: Kansas Geological Survey Bulletin 189.

APPENDIX A

Increased signal-to-noise ratios and higher frequencies have been observed when shot holes are located in the ditch rather than on the road. It would be advantageous to have an auger that could be easily driven into ditches or into any off-road environment. Two people, one to run the auger and one to drive the truck, are needed to drill shot holes with the Giddings. A new piece of equipment has recently made it possible for one person to drill shot holes faster than was previously possible with two people. A new Yamaha all-terrain fourwheeled vehicle (Terrapro) equipped with a hydraulic auger was purchased by the KGS in the Fall of 1987. Originally the auger was set up for drilling fencepost holes. Replacing the auger bit with a 2-in diameter bit made a maneuverable one-person man auger rig. The Terrapro broke down several times during fieldwork for this study and during other projects. The factory redesigned the hydraulic system for more rugged use, making the Terrapro more reliable for drilling shot holes.

The Terrapro was used during the collection of line 4, making only three crew members necessary. The advantages are (1) shot holes can be drilled faster by one person than by two people operating the trailered auger (saving time and money); (2) the Terrapro can be driven into more hard-to-reach places, such as ditches and wooded areas; (3) the environmental impact of the Terrapro is less when shot holes have to be drilled in sensitive areas; (4) besides drilling the shot holes, the Terrapro can be used to shuttle equipment up and down the line quickly and with little environmental impact when working in sensitive areas.

APPENDIX B

Acquisition parameters common to all data.

Seismograph: Input/Output DHR 2400

Source: downhole .50 cal. rifle

Spread Geometry: end-on

Anti-alias filter: 3000 Hz

CDP Acquisition Parameters

Line number	1	2	3	4
Low-cut	220	220	220	110
High-cut	1000	1000	1000	250
Sample rate	0.25 ms	0.25 ms	0.25 ms	0.50 ms
Record length	250 ms	250 ms	250 ms	500 ms
Receivers	2-100 Hz	3-40 Hz	3-40 Hz	3-40 Hz
Receiver array	1.5 ft IL	2 ft PL	2 ft IL	2 ft IL
Receiver spacing	2.5 m	3 m	2 m	4 m
Min. offset	15 m	27 m	12 m	92 m
Max. offset	72.5 m	96 m	58 m	184 m